T cell receptor–targeted immunotherapeutics drive selective in vivo HIV- and CMV-specific T cell expansion in humanized mice

Mengyan Li,[1,2] Scott J. Garforth,[3] Kaitlyn E. O'Connor,[1,2] Hang Su,[1] Danica M. Lee,[1] Alev Celikgil,[3] Rodolfo J. Chaparro,[4] Ronald D. Seidel,[4] R. Brad Jones,[5] Ravit Arav-Boger,[6] Steven C. Almo,[3] and Harris Goldstein[1,2]

[1]Department of Microbiology and Immunology, [2]Department of Pediatrics, and [3]Department of Biochemistry, Albert Einstein College of Medicine, New York, New York, USA. [4]Cue Biopharma, Cambridge, Massachusetts, USA. [5]Division of Infectious Diseases, Department of Medicine, Weill Cornell Medical College, New York, New York, USA. [6]Department of Pediatrics, Division of Infectious Diseases, Medical College of Wisconsin, Milwaukee, Wisconsin, USA.

To delineate the in vivo role of different costimulatory signals in activating and expanding highly functional virus-specific cytotoxic CD8+ T cells, we designed synTacs, infusible biologics that recapitulate antigen-specific T cell activation signals delivered by antigen-presenting cells. We constructed synTacs consisting of dimeric Fc-domain scaffolds linking CD28- or 4-1BB–specific ligands to HLA-A2 MHC molecules covalently tethered to HIV- or CMV-derived peptides. Treatment of HIV-infected donor PBMCs with synTacs bearing HIV- or CMV-derived peptides induced vigorous and selective ex vivo expansion of highly functional HIV- and/or CMV-specific CD8+ T cells, respectively, with potent antiviral activities. Intravenous injection of HIV- or CMV-specific synTacs into immunodeficient mice intrasplenically engrafted with donor PBMCs markedly and selectively expanded HIV-specific (32-fold) or CMV-specific (46-fold) human CD8+ T cells populating their spleens. Notably, these expanded HIV- or CMV-specific CD8+ T cells directed potent in vivo suppression of HIV or CMV infections in the humanized mice, providing strong rationale for consideration of synTac-based approaches as a therapeutic strategy to cure HIV and treat CMV and other viral infections. The synTac platform flexibility supports facile delineation of in vivo effects of different costimulatory signals on patient-derived virus-specific CD8+ T cells, enabling optimization of individualized therapies, including HIV cure strategies.

Introduction

Naive T cells are activated and expanded by 3 coordinated signals elicited by antigen-presenting cells (APCs): signal 1, an antigen-specific signal provided by TCR recognition of its cognate peptide/MHC complex (1); signal 2, a costimulatory signal conveyed through one of several receptors such as CD28, 4-1BB, or OX-40 (2); and signal 3, a proliferation and differentiation signal conferred by cytokines such as IL-2, IL-7, IL-12, and IFN-α/β (3–5). The costimulatory signal is crucial for the activation of naive T cells, as an antigen-specific signal delivered to a naive T cell without a costimulatory signal induces clonal anergy, which restricts subsequent T cell proliferation (6). Multiple strategies have focused on delivering the

requisite stimulatory signal 1 and costimulatory signal 2 using artificial APCs (aAPCs) consisting of transfected K562 cells (7, 8), beads (9), nanoparticles (10–12), or lipid bilayer scaffolds (13). aAPCs are limited to stimulation of ex vivo T cell expansion with removal prior to in vivo administration of the expanded cells, and they cannot be administered as an in vivo immunotherapeutic to stimulate and expand patients' endogenous or adoptively transferred antigen-specific T cells. Herein, we describe the design and application of a unique class of engineered immunomodulatory protein biologics compatible with intravenous administration. We term these biologics artificial immunological synapse for T cell activation, or synTacs (or Immuno-STATs, for selective targeting and alteration of T cells), because they are engineered to recapitulate the antigen-specific and costimulatory signals experienced at the immunological synapse. We hypothesized that by utilizing a modular architecture of covalently tethered peptide-MHC modules (c-pMHC) and costimulatory molecules linked to an Fc domain scaffold, the synTacs could provide a highly flexible platform capable of rapid and efficient ex vivo and in vivo epitope-specific delivery of a wide range of costimulatory, inhibitory, or cytokine signals to TCR-targeted T cell populations. Consequently, the synTac architecture should enable delineation of the mechanisms underlying the divergent functional and molecular effects of different costimulatory signals.

We further postulated synTacs could be effective immunotherapeutics, which direct the specific in vivo activation and expansion

of virus-specific T cell responses. This strategy could contribute to overcoming the major barrier preventing the functional cure of HIV-infected individuals: the recurrence of systemic infection manifested by viremia because of the inability of the intrinsic anti-HIV T cell immune response to effectively eliminate reactivated latently infected cells after the cessation of antiretroviral therapy (ART) (1, 14). The inability of HIV-specific CD8+ T cells (CTLs) to control HIV infection may be reversible, as indicated by in vitro studies reporting restoration of the function of CTLs from HIV-infected individuals by ex vivo antigen-specific stimulation (15) or incubation with dendritic cells loaded with HIV-derived peptides (16). This strategy is further supported by the promising results obtained after infusion of ex vivo–expanded, HIV-specific T cells to treat and provide sustained remission from HIV infection (17). Treatments that mobilize potent HIV-specific immune responses capable of eliminating reactivated latently infected cells will likely need to be combined with latency reversing agents (LRAs) to realize a functional cure for HIV (14).

Herein, we demonstrate that HIV or CMV synTacs, linked to an anti-CD28 scFv or 4-1BBL, or with no costimulatory ligand, selectively and potently stimulated the ex vivo and in vivo expansion of primary HIV- or CMV-specific human CD8+ T cells capable of substantially suppressing ex vivo and in vivo HIV or CMV infection, respectively. These findings validate the application of synTacs for studying the functional impact of different costimulatory signals and their potential broad immunotherapeutic application for the specific in vivo amplification of CD8+ T cell responses and treatment of HIV, CMV, and other viral infections.

Results

Design and production of synTac biologics linking peptide-loaded MHC class I and costimulatory molecules. We evaluated multiple linker and spacer characteristics to identify a well-behaved protein architecture encoded by a single multi-gene vector enabling efficient production of stable synTacs capable of delivering antigen-specific and costimulatory signals to CD8+ T cells. This architecture consists of a c-pMHC module to provide antigen-specificity, and a GCGASGGGGSGGGGS linker to covalently tether an antigenic peptide to β2 microglobulin (β2M). This module is further linked to the HLA-A*0201 MHC heavy chain by an engineered disulfide bond between the cysteine at position 2 of the above linker and a Y84C mutation in the MHC heavy chain (18). This modular design enables synTacs to be readily designed with any peptide and any MHC class I molecule. We used the HLA-A*0201 MHC for initial proof-of-concept studies of the immunostimulatory activity of synTacs because it is the most prevalent MHC class I allele in the North American population (19). Covalent tethering of the peptide supports its physiologically relevant presentation in the MHC heavy chain cleft and binding to its cognate TCR, while preventing exchange with self-peptides that could activate autoreactive T cells. HLA-A*0201 MHC synTacs were constructed with 2 HLA-A*0201–restricted peptides: the HIV Gag SL9 peptide (amino acids [77]SLYNTVATL[85]; ref. 20) or the CMV pp65 peptide (amino acids [495]NLVPMVATV[503]; ref. 21). The β2M C-terminus is covalently joined by a (G4S)[5] linker to the N-terminus of either a single-chain variable fragment (scFv) specific for CD28 (αCD28; ref. 22), an engineered single-chain trimeric 4-1BBL costimulatory ligand capable of activating the 4-1BB costimulatory pathway (23), or a control FLAG

epitope, which only stimulates the TCR (signal 1). The MHC heavy chain C-terminus is fused to a C-terminally His[8]-tagged unmutated human IgG1 CH2-CH3 domain homodimer (Fc domain) to generate a bivalent dimeric molecule with sufficient avidity for T cell binding and activation (Figure 1A and Supplemental Table 1; supplemental material available online with this article; https://doi.org/10.1172/JCI141051DS1). After transfection of FreeStyle 293-F cells with the indicated vector, synTac proteins secreted by the transfected cells were purified by metal affinity and size exclusion chromatography (Figure 1B). SynTac proteins were validated by SDS-PAGE under reducing conditions by visualization of the predicted subunits (Figure 1C) and were highly stable, with no perceptible loss of activity during 6 months of storage at 4°C. To determine whether the 4-1BBL covalent trimer possessed binding activity for 4-1BB, we examined binding to CD8+ TCR[neg] Jurkat/MA cells transduced with a 4-1BB–encoding lentiviral vector (Figure 1D). pp65-4-1BBL and SL9-4-1BBL synTacs bound to more than 90% of the 4-1BB–expressing Jurkat/MA cells, compared with minimal binding by the SL9- and pp65-synTacs bearing αCD28 or FLAG (Figure 1E). In the absence of expression of a TCR specific for SL9 or pp65, binding of the pp65-4-1BBL or SL9-4-1BBL synTacs did not activate the nuclear factor of activated T cells–regulated (NFAT-regulated) luciferase reporter gene in the Jurkat/MA cells (Figure 1F).

SL9-synTacs selectively bind and activate SL9-specific TCRs. SL9-synTac binding and activity were examined using CD8+ TCR[neg] Jurkat/MA cells expressing an SL9-specific TCR after transduction with a lentivirus encoding SL9-specific TCR and GFP genes as described (24, 25). Flow cytometric analysis demonstrated binding to SL9-specific, TCR-expressing Jurkat/MA cells by SL9-αCD28-synTac (>90%), SL9-4-1BBL-synTac (>90%), and SL9-FLAG-synTac (>55%), but not by αCD28, 4-1BBL, or FLAG-linked pp65-synTac (Figure 1G). In contrast, neither SL9-synTac nor pp65-synTac bound to Jurkat/MA cells expressing a TCR specific for an irrelevant peptide, HIV KK10 ([263]KRWIILGLNK[272]; ref. 24 and Figure 1G). SL9-αCD28-synTac or SL9-4-1BBL-synTac, but not pp65-αCD28-synTac or pp65-4-1BBL-synTac, substantially activated the NFAT-regulated luciferase reporter gene in the SL9-specific, TCR-transduced Jurkat/MA cells in a dose-responsive manner. Only the highest dose (200 nM) of SL9-FLAG-synTac stimulated luciferase production by the SL9-specific, TCR-transduced Jurkat/MA cells, which was comparable to that elicited by a greater than 200-fold lower concentration of SL9-αCD28-synTac (0.8 nM; Figure 1H). The decreased stimulatory capacity of the SL9-FLAG-synTac may be related to its reduced binding to the SL9-specific, TCR-expressing Jurkat/MA cells (~55%) as compared with the binding of SL9-αCD28-synTac and SL9-4-1BBL-synTac (>90%) or to its lack of a costimulatory signal activator (Figure 1G).

The ability of synTacs to deliver antigen-specific and costimulatory signals was evaluated with a CD8+ T cell clone derived as described (26), which expresses an SL9-specific TCR (Figure 2A). SL9-αCD28-synTac and SL9-4-1BBL-synTac, but not SL9-FLAG-synTac or pp65-synTac, potently stimulated IFN and TNF production (Figure 2B) and degranulation, as indicated by CD107a expression (Figure 2C). The contribution of costimulatory signaling to CD8+ T cell clone activation was further demonstrated by the enhanced proliferation of the SL9-specific CD8+ T cell clone stimulated by SL9-αCD28-synTac and SL9-4-1BBL-synTac as compared with the
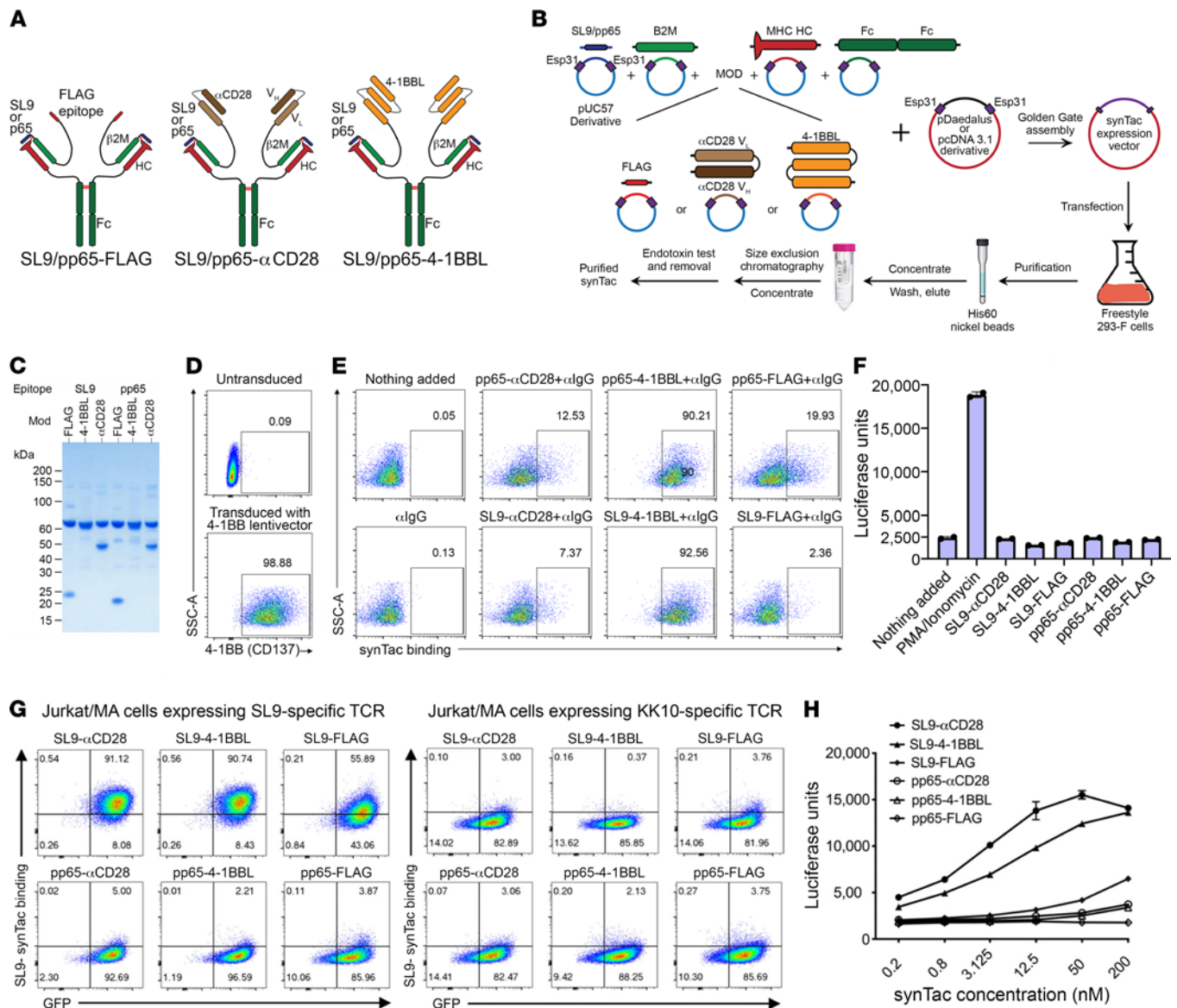
Figure 1. Structural representation of synTac proteins and their production and functional activity. (**A**) SynTacs were constructed as a split sc-pMHC-Fc fusion, with the β2M and the MHC HLA-A*0201 alpha chain linked through engineered interchain disulfide bonds, and the FLAG, αCD28, or 4-1-BBL domains linked to the β2M carboxy end. (**B**) Outline of protocol for production of SL9- or pp65-FLAG, -αCD28, and -4-1BBL synTacs. (**C**) SDS-PAGE gel showing the molecular weights of the reduced synTacs. (**D**) 4-1BB expression on Jurkat/MA cells that were transduced with a 4-1BB–encoding lentiviral vector. (**E**) Quantification of synTac (1 nM) bound to 4-1BB–expressing Jurkat/MA cells. (**F**) 4-1BB–expressing Jurkat/MA cells that express an NFAT-driven luciferase reporter were incubated with synTac constructs (100 nM) or stimulated with PMA/ionomycin. After overnight incubation, luciferase activity was measured. (**G**) Jurkat/MA cells were transduced with a lentivector encoding a TCR specific for either SL9 (left) or KK10 (right), incubated with the indicated synTac molecules (1.56 nM) for 30 minutes, and bound synTac molecules were detected by flow cytometry. (**H**) Luciferase activity was quantified after overnight incubation of SL9-TCR–transduced Jurkat/MA cells with synTac molecules (0.2 nM to 200 nM).

SL9-FLAG-synTac, with no appreciable proliferation induced by pp65-specific synTacs (Figure 2D).

To evaluate the ability of SL9-synTac–delivered TCR (signal 1) and costimulatory molecule (signal 2) activation to stimulate antigen-specific expansion of primary CD8+ T cells, we isolated PBMCs containing SL9-specific CD8+ T cells from 4 HIV-seropositive HLA-A*0201 donors. Twelve days after in vitro treatment with one dose of SL9- or pp65-specific synTacs, SL9-specific CD8+ T cells were quantified by flow cytometric analysis of CD8 expression and HLA-A*0201 tetramer binding as described (25). A representative dot plot is shown in Figure 3A. As compared with untreated PBMCs and pp65-specific-synTac–treated PBMCs, treatment with SL9-αCD28-synTac, SL9-4-1BBL-synTac, and SL9-FLAG-synTac increased by up to 17.5-fold, 7.9-fold, and 7.2-fold, respectively—the fraction of SL9-specific CD8+ T cells in the 4 donors (Figure 3B). Although delivery of the TCR signal 1 and the CD28 costimulatory signal 2 by the SL9-αCD28-synTac was the most potent stimulator of SL9-specific CD8+ T cells ($P = 0.0401$), of great interest was the expansion of SL9-specific CD8+ T cells induced by SL9-FLAG-synTac delivering the TCR signal 1 alone without a costimulatory signal 2. Analysis of
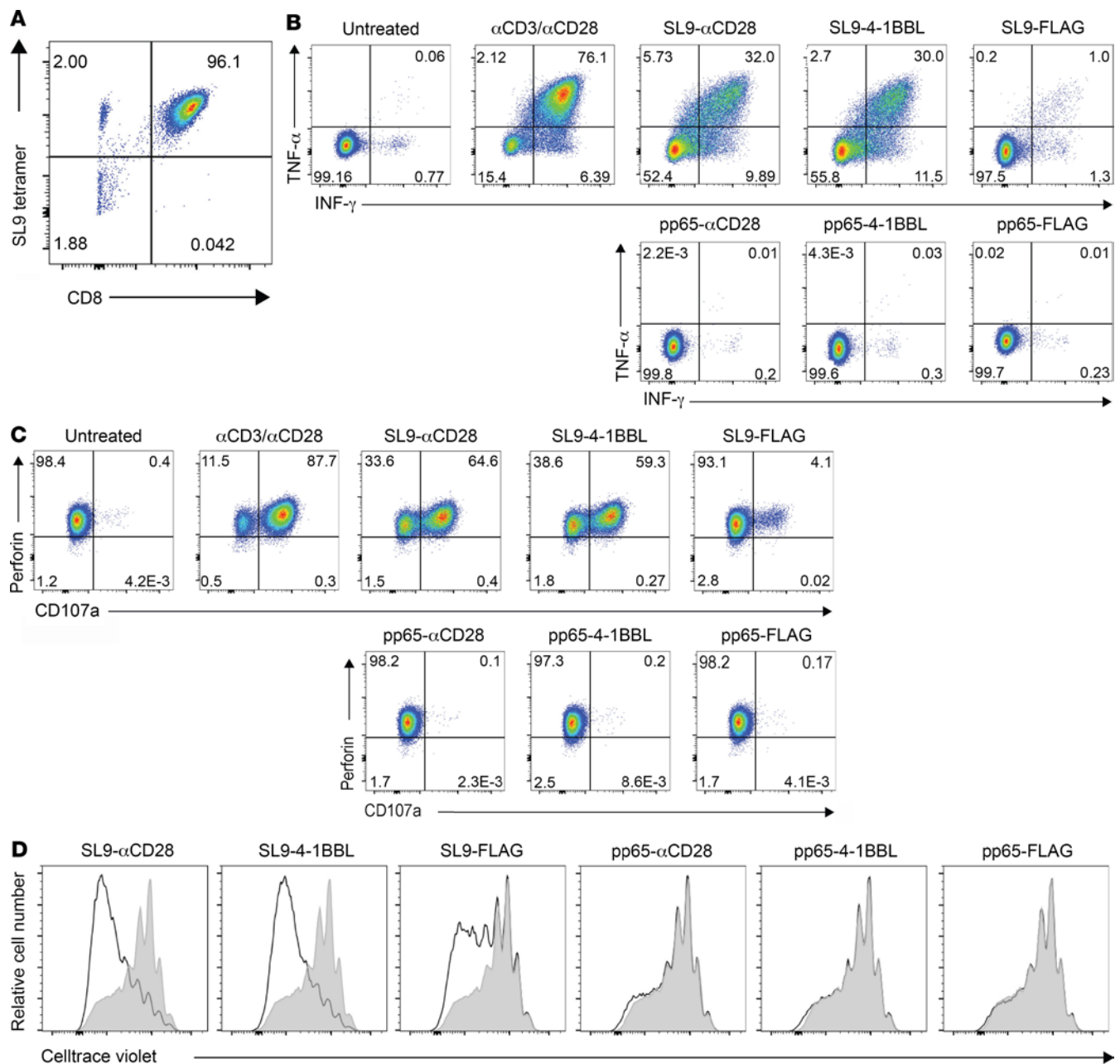
Figure 2. synTac stimulation of an SL9-specific CD8⁺ T cell clone. (**A**) SL9 tetramer staining of the SL9-specific CTL clone. (**B** and **C**) The SL9-specific CTL clone was untreated or treated overnight with anti-CD3/anti-CD28 or the indicated synTacs (100 nM) and analyzed for intracellular expression of (**B**) IFN-γ and TNF-α and (**C**) the degranulation marker CD107a and perforin. (**D**) The SL9-specific CTL clone was stained with Cell Trace Violet (0.25 μM), treated with the indicated synTac (100 nM), cultured for 6 days in complete RPMI with added IL-2 (50 U/mL), and cellular proliferation was determined by flow cytometric analysis of cellular dye dilution.

costimulatory molecule expression by the SL9-specific CD8⁺ T cells from 3 donors (OM265, HGLK9, and CIRC0145) prior to SL9-synTac stimulation demonstrated greater expression of CD28 (ranging from 15.5% to 59.5%) than 4-1BB (ranging from 0% to 14.2%), primarily expressed by activated T cells (Figure 3C and ref. 27).

We evaluated the functional activity of SL9-specific CD8⁺ T cells expanded by SL9-synTac treatment by quantifying polyfunctional cytokine production, a phenotype associated with improved protective immunity after vaccination or natural infection (28). We gated for CD8⁺SL9 tetramer-binding T cells (Supplemental Figure 1A) and assessed IFN-γ, TNF-α, and CD107a expression as shown

in representative dot plots (Supplemental Figure 1B). Greater than 80% of the SL9-αCD28-synTac–, SL9-4-1BBL-synTac–, and SL9-FLAG-synTac–expanded SL9-specific CD8⁺ T cells expressed IFN-γ, TNF-α, and CD107a after SL9 peptide-loaded T2 cell–stimulation as compared with minimal cytokine expression detected after stimulation with control IV9 peptide-loaded T2 cells (Figure 3D). Interestingly, expansion and cytokine production in response to SL9-synTac treatment did not correlate with the initial level of CD28 or 4-1BB expression prior to SL9-synTac treatment. To test the capacity of SL9-synTac–expanded CD8⁺ T cells to inhibit HIV infection, we super-infected PBMCs from one of the HIV-seropositive donors
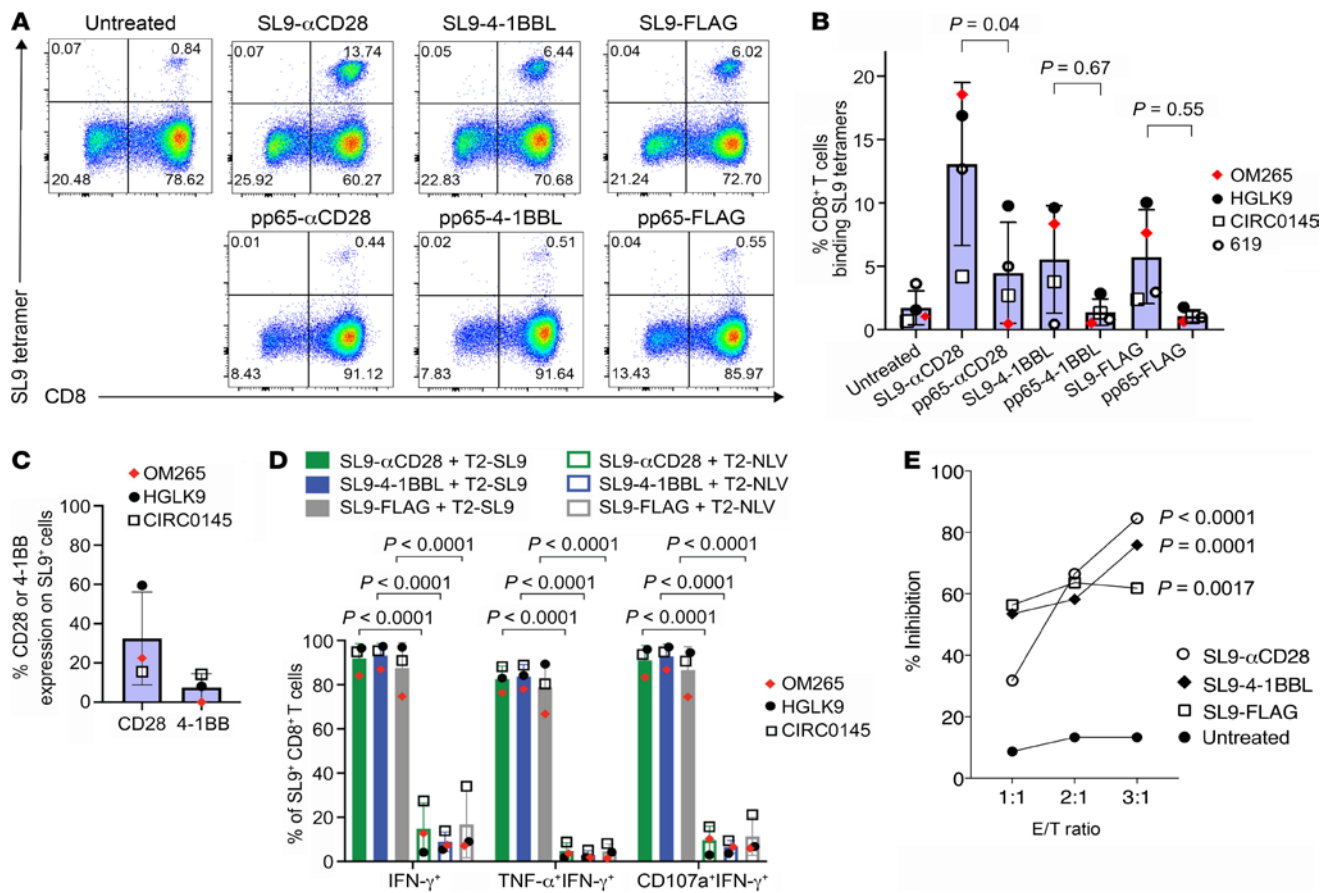
Figure 3. SL9-synTac treatment stimulated in vitro expansion of functional SL9-specific CD8+ T cells from HLA-A*0201 HIV-infected donors. (**A**) HIV-seropositive donor (donor OM265) PBMCs treated with the indicated synTacs (0.1 nM) were cultured for 12 days in complete RPMI media with IL-2 (100 U/mL) and Raltegravir (1 μM), and analyzed by flow cytometry. (**B**) Summary data from 4 different HIV-infected donors (individual donors denoted as OM265, HGLK9, CIRC0145, and 619) treated with the indicated pp65- or SL9-synTacs. Data represent mean ± SD, analyzed using a 1-way ANOVA, followed by Tukey's multiple comparisons test. (**C**) Baseline level of CD28 or 4-1BBL expression by SL9-specific CD8+ T cells from the 3 HIV-infected donors shown in **B**. (**D**) Quantification of SL9-αCD28, 4-1BBL, or FLAG synTac-expanded cells expressing IFN-γ, both TNF-α and IFN-γ, or both CD107a and IFN-γ by flow cytometry after stimulation overnight with T2 cells loaded with SL9 or CMV-pp65 peptides in complete IMDM with IL-2 (100 U/mL). (**E**) SL9-specific CD8+ T cells from HIV-seropositive donor 619 expanded by treatment of PBMCs with SL9-αCD28, SL9-4-1BBL, or SL9-FLAG synTac were added to IMC-Bal super-infected autologous PBMCs at E/T ratios of 1:1, 2:1, and 3:1, respectively. Three days later, LucR levels were quantified. An experiment representative of 2 independent experiments is shown. Statistical significance of infection inhibition was determined by percentage of reduction of IMC-Bal–infected PBMC LucR levels in cultures with added untreated cells as compared with synTac-treated cells at an E/T ratio of 3:1 using 2-way ANOVA followed by Sidak's multiple comparison's test.

(donor 619) with an infectious molecular clone of HIV-1 (IMC-LucR) that employs Renilla luciferase (LucR) expression as a surrogate marker for quantifying the level of productive HIV infection (29). Using PBMCs from the same donor (donor 619), we cocultured IMC-LucR–infected PBMCs with untreated PBMCs or SL9-synTac–treated PBMCs and measured LucR. PBMCs with SL9-specific CD8+ T cells expanded by treatment with SL9-αCD28, SL9-4-1BBL, or SL9-FLAG synTacs potently suppressed HIV-1 infection in a dose-responsive manner by up to 85%, 74%, or 61%, respectively, using an E/T ratio of 3:1, as compared with minimal inhibition by the addition of an equivalent number of untreated PBMCs (Figure 3E).

pp65-synTacs stimulate potent in vitro expansion of functional pp65-specific CD8+ T cells. While SL9-specific CD8+ T cell proliferative capacity may be impaired by sustained activation due to chronic HIV infection (30), CMV-specific T cell responses are not affected by chronic HIV infection (28). Furthermore, because CMV infection increases morbidity and mortality in HIV-infected individuals (31,

32), pp65-synTac–stimulated expansion of CMV-specific CD8+ T cells may represent a novel strategy to treat or prevent CMV infection in HIV-infected individuals and other immunosuppressed patients. PBMCs containing pp65-specific CD8+ T cells were obtained from 7 HIV-seropositive HLA-A*0201 donors. PBMCs from 4 of these donors also contained SL9-specific CD8+ T cells. The PBMCs were treated with 1 dose (0.1 nM) of pp65- or SL9-specific synTacs for 12 days and the population of pp65-specific CD8+ T cells was quantified by flow cytometry (Figure 4A). Prior to synTac treatment, the fraction of CD8+ T cells that were pp65-specific from these donors ranged from 1.2% to 5.3%, an amount that significantly increased after treatment with pp65-αCD28-synTac (range 3.6%–54.2%), pp65-4-1BBL-synTac (range 5.2%–46.4%), or pp65-FLAG-synTac (range 2.2%–32.7%), but not after treatment with SL9-synTacs linked to the same costimulatory ligands (Figure 4B). As observed for SL9-specific CD8+ T cells, delivery of the TCR signal 1 and the CD28 costimulatory signal 2 by pp65-αCD28-synTac treatment induced the most
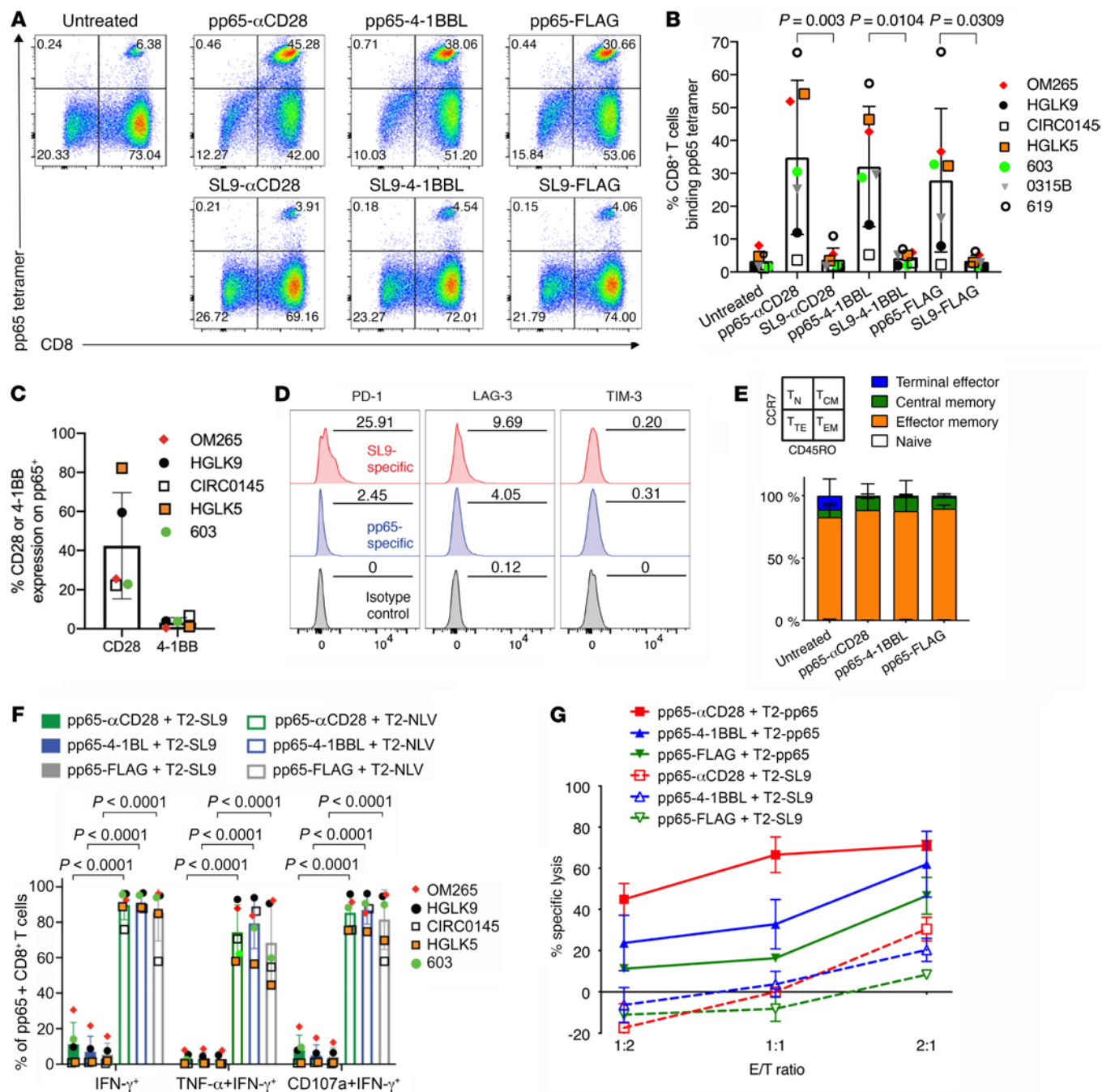
Figure 4. pp65 synTac stimulates in vitro expansion of functional pp65-specific CD8+ T cells from HLA-A*0201 HIV-infected donors. (**A**) PBMCs from HIV-seropositive donor OM265 were treated with the indicated synTacs (0.1 nM), cultured for 12 days in complete IMDM with IL-2 (100 U/mL) and Raltegravir (1 μM) and analyzed by flow cytometry. (**B**) Summary data from 7 different donors (OM265, HGLK9, CIRC0145, HGLK5, 603, 0315B, and 619) of pp65-specific CD8+ T cells after treatment with indicated synTacs are shown as mean ± SD with statistical analysis performed using ordinary 1-way ANOVA followed by Tukey's multiple comparisons test. (**C**) Baseline level of CD28 or 4-1BBL expression from pp65-specific CD8+ T cells of 5 HIV-infected donors shown in **B**. (**D**) PD-1 (left), LAG-3 (middle), and TIM-3 (right) expression on SL9-specific (red shade) or pp65-specific (blue shaded) CD8+ T cells from HIV-seropositive donor 619. The numbers in each panel indicate the percentage positive for each marker compared with the isotype control (gray shaded). (**E**) Frequency of TN (naive, CD45RO−CCR7+), TCM (central memory, CD45RO+CCR7+), TTE (terminal effector, CD45RO−CCR7−), and TEM (effector memory, CD45RO+CCR7−) from pp65-specific CD8+ T cells expanded by pp65-synTac treatment of seropositive donor OM265 PBMCs. Data represent the mean ± SD of 2 independent experiments of this donor. (**F**) Intracellular cytokine expression of pp65-specific CD8+ T cells from 5 different donors expanded by treatment with the indicated synTac that expresses IFN-γ, TNF-α and IFN-γ, or CD107a and IFN-γ after stimulation with pp65- or SL9-peptide–pulsed T2 cells. (**G**) Cytolytic activity of synTac-expanded pp65-specific CD8+ T cells from HIV-seropositive donor HGLK5 directed at pp65- or SL9-peptide–pulsed T2 cells determined using EuTDA cytotoxicity assay cocultured at the indicated E/T ratios. Data shown represent mean ± SD of 3 experimental replicates and 2 independent experiments.

potent expansion of pp65-specific CD8+ T cells, but marked expansion of p65-specific CD8+ T cells was also stimulated by TCR signal 1 alone by pp65-FLAG-synTac. Analysis of CD28 and 4-1BB expression by the pp65-specific CD8+ T cells from 5 donors prior to pp65-synTac stimulation demonstrated greater CD28 expression (range 22.3%–82.2%) than 4-1BB expression (range 0.5%–6.7%; Figure 4C). Interestingly, as observed for PBMCs treated with SL9-synTac (Figure 3, B and C), the degree of expansion was similar across different pp65-synTac treatments and did not correlate with the initial level of CD28 or 4-1BB expression, which may be due to upregulated 4-1BB expression observed after CD8+ T cell stimulation (27). To determine whether the exhaustion phenotype of SL9-specific CD8+ T cells contributed to their reduced SL9-synTac–induced expansion relative to the more robust pp65-synTac–induced expansion of pp65-specific CD8+ T cells, we evaluated the baseline expression of exhaustion markers in SL9-specific and pp65-specific CD8+ T cells in PBMCs from an HIV-seropositive donor (donor 619) possessing distinct CD8+ T cell populations that individually recognize each of the 2 antigens. As compared with pp65-specific CD8+ T cells, the fraction of SL9-specific CD8+ T cells expressing PD-1 and LAG-3 was more than 10-fold higher and more than 2-fold higher, respectively, while TIM-3 expression was similar in both populations (Figure 4D). We also evaluated the memory phenotype of the expanded pp65-specific CD8+ T cells in one HIV-seropositive donor (donor HGLK5) based on differential CD45RO and CCR7 expression (33), and determined that after the substantial expansion induced by treatment with pp65-synTacs, more than 90% of the pp65-specific CD8+ T cells were effector memory T cells (CD45RO+, CCR7−; Figure 4E).

After gating for CD8+ p65 tetramer-binding T cells (Supplemental Figure 1A), we assessed IFN-γ, TNF-α, and CD107a expression by flow cytometry as shown in representative dot plots (Supplemental Figure 1C). Greater than 70% of pp65-αCD28−, pp65-4-1BBL−, or pp65-FLAG-synTac–expanded pp65-specific CD8+ T cells activated by pp65-peptide–loaded T2 cells displayed polyfunctional activity, as indicated by TNF-α, IFN-γ, and CD107a expression, in contrast to the minimal cytokine production induced by SL9-loaded T2 cells (Figure 4F). pp65-specific CD8+ T cells expanded by pp65-synTac stimulation displayed dose-responsive lysis of pp65-loaded T2 cells. The most potent cytotoxic activity was displayed by pp65-αCD28-synTac–stimulated cells, followed by pp65-4-1BBL– and pp65-FLAG-synTac–stimulated cells, while all pp65-synTac–stimulated cells displayed negligible cytolytic activity directed at SL9-loaded T2 cells (Figure 4G).

We also evaluated pp65-synTac stimulation of PBMCs from an HIV-seronegative HLA*0201 donor (donor HGLK055). As shown in representative dot plots, 12 days after single-dose synTac treatment (2.5 nM), the fraction of PBMCs that were pp65-specific CD8+ T cells markedly increased from approximately 0.2% in the untreated PBMCs to approximately 70% (>310-fold), 42% (>185-fold), or 30% (>130-fold) in the pp65-αCD28-synTac–, pp65-4-1BBL-synTac–, or pp65-FLAG-synTac–treated PBMCs, respectively, corresponding to expansion to approximately 80%, 70%, or 55% of the total CD8+ T cell population, respectively (Figure 5A). Pooled data from 4 independent experiments from the same HIV-uninfected donor showed marked expansion of pp65-specific CD8+ T cells by treatment with pp65-synTacs but not by SL9-synTac treatment. Delivery of the TCR signal 1 and CD28 costimulatory signal 2 by the pp65-αCD28-

synTac stimulated significantly greater expansion (P = 0.0118) of pp65-specific CD8+ T cells than the delivery of the TCR signal alone by pp65-FLAG-synTac (Figure 5B). Again, we observed that despite not delivering a costimulatory signal, treatment with pp65-FLAG-synTac markedly expanded primary pp65-specific CD8+ T cells. We addressed the possibility that this was due to costimulatory signals delivered by adjacent activated human APCs in the PBMCs by determining whether pp65-FLAG-synTac treatment of highly purified CD8+ T cells also expanded the pp65-specific CD8+ T cell population. Accordingly, highly purified CD8+ T cells isolated from HGLK055 donor PBMCs using a CD8+ T cell isolation kit (Miltenyi Biotec) were treated with the indicated pp65-synTac for 12 days (Supplemental Figure 2). The CD8+ T cell population purity was demonstrated by analysis for CD3 and CD4 expression (Supplemental Figure 2A) and APC-marker CD14 and CD56 expression (Supplemental Figure 2B). pp65-FLAG-synTac treatment of the highly purified CD8+ T cells markedly expanded the pp65-specific CD8+ T cell population, indicating that synTac function, particularly pp65-FLAG-synTac, is not dependent on the presence of APCs (Supplemental Figure 2C).

pp65-synTac potency was demonstrated by the marked expansion of pp65-specific CD8+ T cells in PBMCs from donor HGLK055 by concentrations of pp65-αCD28-synTac, pp65-4-1BBL-synTac, or pp65-FLAG-synTac as low as 0.004 nM; pp65-αCD28-synTac consistently afforded the most potent expansion of pp65-specific CD8+ T cells across a wide range of doses (Figure 5C). One dose of pp65-αCD28-synTac, pp65-4-1BBL-synTac, or pp65-FLAG-synTac (2.5 nM) stimulated rapid expansion of pp65-specific CD8+ T cells, with the fraction of pp65-specific CD8+ T cells expanding from approximately 1% to approximately 40% by 7 days and to approximately 70% to 80% by 12 days after treatment (Figure 5D). Four days after treatment of the PBMCs with pp65-synTacs, increased production of IFN-γ (Figure 5E), granzyme B (Figure 5F), MIP-1β (Figure 5G), and perforin (Figure 5H) was detected in the culture supernatant, which further increased by 7 days after pp65-synTac treatment. pp65-specific CD8+ T cells in PBMCs from the same donor (donor HGLK055) expanded by pp65-αCD28-synTac, pp65-4-1BBL-synTac, or pp65-FLAG-synTac treatment were predominately effector memory T cells (Figure 6A). In addition, as shown in representative dot plots, the pp65-specific CD8+ T cells expanded by pp65-synTac treatment displayed polyfunctional cytokine activity, as indicated by production of TNF-α, IFN-γ, and CD107a after stimulation with pp65-peptide–loaded T2 cells (Figure 6B), but not after stimulation with SL9-peptide–loaded T2 cells (Figure 6C). After challenge with pp65-peptide–loaded T2 cells, approximately 95% of the pp65-αCD28-synTac–, pp65-4-1BBL-synTac–, or pp65-FLAG-synTac–expanded pp65-specific CD8+ T cells expressed IFN-γ, while almost 25% of the cells displayed polyfunctional IFN-γ, TNF-α, and CD107a responses (Figure 6D). By comparison, after challenging with SL9-peptide–loaded T2 cells, a far smaller fraction of the pp65-synTac–expanded CD8+ T cells expressed IFN-γ (8%–21%), both TNF-α and IFN-γ (<1%), or IFN-γ, TNF-α, and CD107a (<1%; Figure 6D). The pp65-specific CD8+ T cells expanded by pp65-synTacs, particularly those treated with pp65-αCD28-synTac, displayed dose-responsive cytolytic activity directed at pp65-peptide–loaded T2 cells, as compared with minimal cytolysis of SL9-peptide–loaded T2 cells (Figure 6E). We evaluated CMV infection inhibition by pp65-specific CD8+ T cells expanded by pp65-synTac treatment.
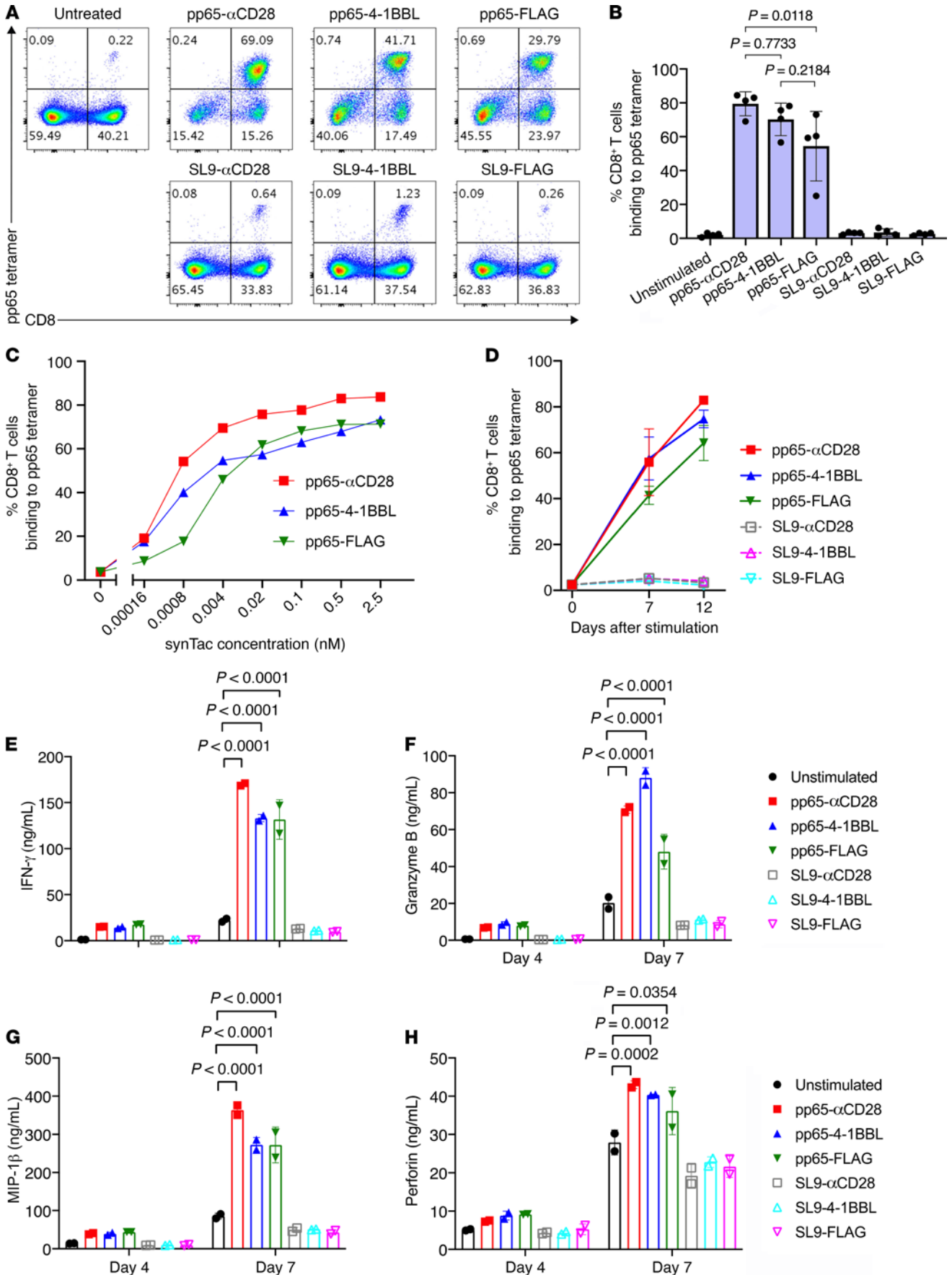
Figure 5. pp65 synTac treatment potently stimulates in vitro expansion of functional pp65-specific CD8+ T cells in an HIV-seronegative donor. (**A**) HGLK055 PBMCs were treated with the indicated synTac (2.5 nM), cultured for 12 days in complete RPMI media with IL-2 (100 U/mL), and analyzed by flow cytometry. (**B**) Results from 4 independent experiments as described in **A** showing percentage of pp65-specific CD8+ T cells 12 days after PBMCs from donor HGLK055 were treated with synTacs; mean ± SD are shown and statistical significance was assessed by ordinary 1-way ANOVA followed by Tukey's multiple comparisons test. (**C**) The percentage of pp65-specific CD8+ T cells 12 days after treatment of HGLK055 PBMCs with the indicated synTac doses and cultured in complete IMDM with IL-2 (100 U/mL). Data shown are representative of 2 independent experiments. (**D**) HGLK055 PBMCs were treated with the indicated synTacs (2.5 nM) and percentage of pp65-specific CD8+ T cells was determined after 7 and 12 days after culture in complete media with IL-2 (100 U/mL). Data shown represent mean ± SD of 3 independent experiments. (**E**–**H**) After 4 days and 7 days of culture as described in **D**, cell culture supernatant was analyzed using the MILLIPLEX Multiplex assay to quantify concentrations of (**E**) IFN-γ, (**F**) granzyme B, (**G**) MIP-1β, and (**H**) perforin. Data represent mean ± SD of replicate samples and were analyzed using a 2-way ANOVA, followed by Tukey's multiple comparisons test.

Untreated PBMCs or PBMCs with their pp65-specific CD8+ T cells expanded by 7 days of treatment with pp65-synTacs or SL9-synTacs were added to HLA-A*0201 fibroblasts (MRC-5 cells) and infected with a recombinant pp28-Towne strain of human CMV expressing luciferase (CMV-luc) under the control of the true late pp28 gene. This system provides a surrogate to evaluate the capacity of antiviral agents to inhibit CMV during one full replication cycle (34, 35), which highly correlates with the CMV plaque infection assay (35). In contrast to SL9-synTac–treated PBMCs, which did not significantly suppress luciferase activity, pp65-synTac–treated PBMCs displayed highly significant suppression of luciferase activity in MRC-5 cells infected with CMV-luc (MOI = 3) as indicated by near-complete suppression of infection by pp65-synTac–expanded PBMCs at a E/T ratio of 1:2 (Figure 6F). With a reduced E/T ratio of 1:5, pp65-αCD28-synTac–stimulated PBMCs completely suppressed CMV-luc infection, while pp65-4-1BBL-synTac– and pp65-FLAG-synTac–stimulated PBMCs displayed a reduced capacity to suppress CMV-luc infection (Figure 6G).

Potent in vivo expansion of functional pp65- and SL9-specific CD8+ T cells by pp65-peptide– or SL9-peptide–targeting synTacs. We determined the in vivo synTac pharmacokinetics by measuring sequential serum levels after intravenous injection of pp65-4-1BBL-synTac (Figure 7A). While the pp65-synTac half-life was relatively short (~3 hours), the potent in vitro activity of synTac at ≤ 0.1 nM suggests that administration of one dose of synTac (4 mg/kg) should provide sustained in vivo stimulation of targeted T cells for at least 12 hours. We examined the capacity of synTacs to stimulate in vivo expansion of the pp65- or SL9-specific CD8+ T cell populations using an NSG humanized mouse model we established (29, 36). After intrasplenic injection of PBMCs from HGLK055, the HIV-seronegative HLA*0201 donor used for in vitro studies (Figures 5 and 6), mice were left untreated or intravenously injected with 1 dose (4 mg/kg) of the indicated pp65-synTacs or SL9-synTacs. One week later, the pp65-specific CD8+ T cell population in their spleens was measured by flow cytometry (Figure 7B). As shown in representative dot plots, pp65-synTac treatment of humanized mice markedly expanded the fraction of human pp65-specific CD8+ T cells in their spleens

as compared with untreated and SL9-synTac–treated mice (Figure 7C). Pooled results from multiple experiments demonstrated that, compared with untreated mice (*n* = 11), mice treated with pp65-αCD28-synTac (*n* = 7), pp65-4-1BBL-synTac (*n* = 7), or pp65-FLAG-synTac (*n* = 5) exhibited significant 28-fold (*P* < 0.0001), 16-fold (*P* = 0.002), or 22-fold (*P* < 0.0001) expansion of the pp65-specific fraction of CD8+ T cells, respectively, from a mean precursor frequency of less than 1% in the untreated mouse spleens to a mean of approximately 25%, 14%, or 20%, respectively (Figure 7D). The pp65-αCD28-synTac–elicited expansion was significantly greater (*P* = 0.0056) than pp65-4-1BBL-synTac–stimulated expansion, but statistically indistinguishable from the pp65-FLAG-synTac treatment. pp65-specific CD8+ T cell expansion in mouse spleens induced by pp65-synTac treatment was significantly greater than the negligible expansion induced by SL9-synTacs linked to comparable costimulatory ligands αCD28 (*P* < 0.0001), 4-1BBL (*P* = 0.0063), or FLAG (*P* = 0.0006) (Figure 7, C and D). The majority of the pp65-tetramer–positive CD8+ T cells untreated with pp65-synTac were effector memory T cells (Figure 6A), which may expand after stimulation with antigen-specific TCR signals alone, consistent with the ability of pp65-FLAG-synTac, which lacks costimulatory functionality, to elicit significant expansion. After treatment with pp65-αCD28-synTac, pp65-4-1BBL-synTac, or pp65-FLAG-synTac, more than 90% of the pp65-synTac–expanded pp65-specific CD8+ T cells had an effector memory CD8+ T cell phenotype, indicating selective in vivo expansion or differentiation of the effector memory population after pp65-synTac treatment (Figure 7E). Utilizing PBMCs from an HIV-seropositive donor (donor 619) possessing distinct CD8+ T populations that individually recognize either HIV-SL9 and CMV-pp65, we compared the in vivo capacity and selectivity of SL9-αCD28-synTac or pp65-αCD28-synTac to stimulate expansion of intrasplenically injected SL9- or pp65-specific CD8+ T cells, respectively, in the spleens of NSG mice. Representative dot plots (Figure 7F) and a pooled data set (Figure 7G) demonstrated that compared with untreated mice, treatment with SL9-αCD28-synTac significantly expanded (*P* < 0.001) the fraction of SL9-specific CD8+ T cells by 32-fold, from a mean precursor frequency of 0.6% to 21.8%, while pp65-αCD28-synTac treatment had a negligible effect. pp65-αCD28-synTac treatment of mice from the HIV-infected donor significantly expanded (*P* = 0.018) the fraction of pp65-specific CD8+ T cells as compared with untreated mice by 8.3-fold, from a mean of 5.5% to 45.9%, while SL9-αCD28-synTac treatment had a negligible effect (Figure 7, H and I). The predominant phenotype of the SL9-specific CD8+ T cells or pp65-specific CD8+ T cells expanded by treatment with SL9-αCD28-synTac or pp65-αCD28-synTac, respectively, was that of effector memory T cells (Figure 7J). These observations further illustrated the potency and selectivity of synTac constructs for driving in vivo expansion of epitope-specific CD8+ T cells from the same donor.

Evaluation of the capacity of CD8+ T cells expanded by in vivo treatment with synTacs to suppress in vivo CMV and HIV infection. We examined the in vivo capacity of pp65-specific CD8+ T cells to suppress CMV infection by developing a strategy guided by observations that it takes at least 1 week for intravenously injected pp65-αCD28-synTac to stimulate significant in vivo expansion of pp65-specific CD8+ T cells in the mouse spleens and that CMV-luc infection of MRC-5 cells rapidly peaks approximately 3 to 4 days after infection.
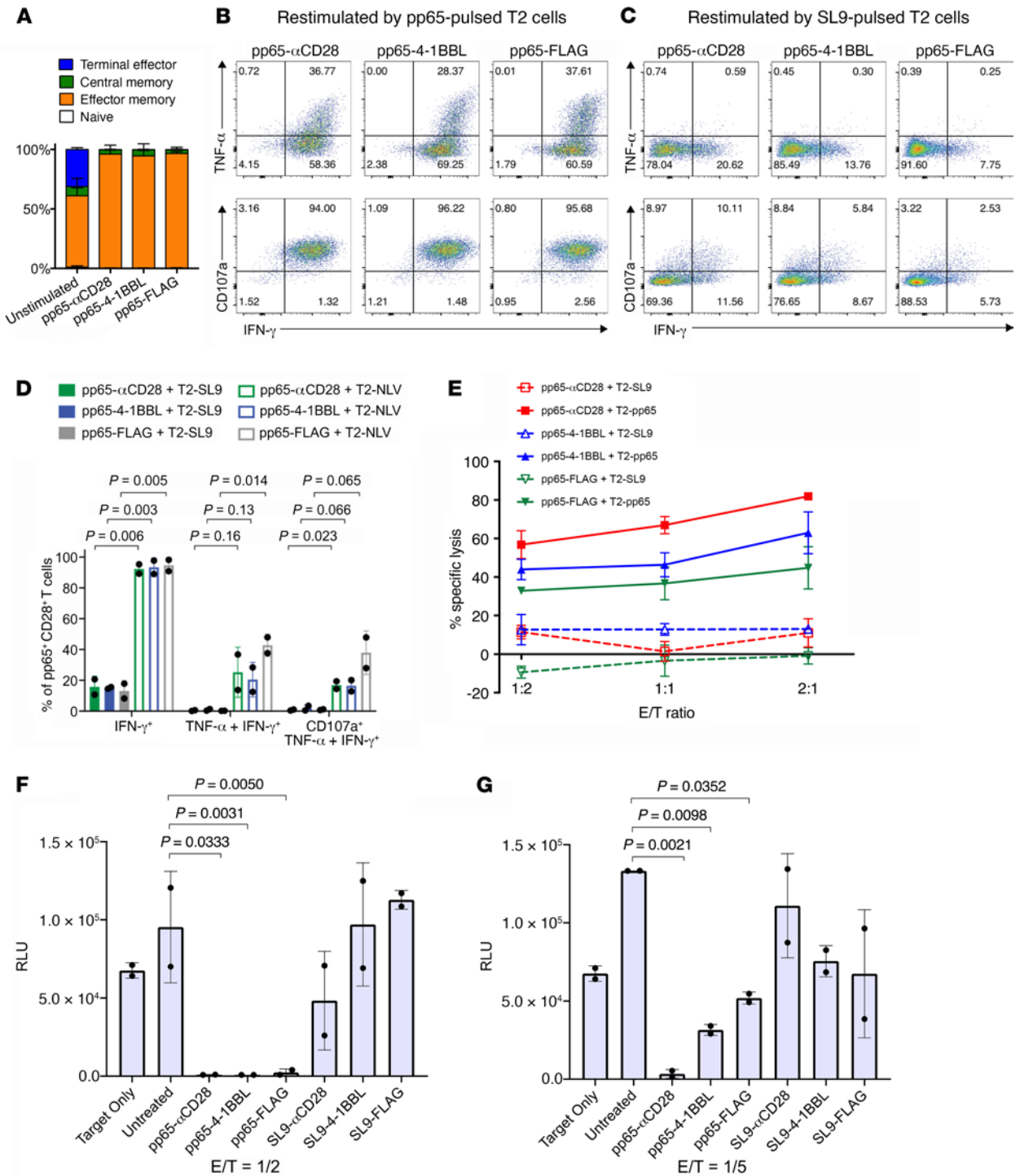
Figure 6. pp65-synTac expanded pp65-specific CD8⁺ T cells from a HIV-seronegative donor are polyfunctional and potently inhibit CMV infection. (**A**) Frequency of pp65-specific cells that are TN, TCM, TTE, and TEM. Data represent 2 independent experiments showing mean ± SD. (**B** and **C**) Intracellular cytokine staining of IFN-γ and TNF-α (upper panels) or CD107a and IFN-γ (lower panels), in pp65-specific CD8⁺ T cells expanded by treatment with the indicated synTac after overnight stimulation with (**B**) pp65- or (**C**) SL9-pulsed T2 cells. Dot plots shown were gated from the pp65-tetramer⁺ population and are representative of 2 independent experiments. (**D**) Quantification of cells that express IFN-γ, TNF-α and IFN-γ, TNF-α, and IFN-γ and CD107a combined from 2 independent experiments showing mean ± SD and statistically analyzed using ordinary 1-way ANOVA followed by Tukey's multiple comparisons test. (**E**) Twelve days after treatment with the indicated synTac, cytolytic activity directed at pp65- or SL9-peptide–pulsed T2 cells was evaluated after 4-hour culture at the indicated E/T ratios using an EuTDA cytotoxicity assay. Data shown represent mean ± SD of 3 experimental replicates and are representative of 2 independent experiments. (**F** and **G**) PBMCs treated with the indicated synTac (0.1 nM) for 7 days were cocultured with HLA-A*0201–expressing human fibroblasts infected with a recombinant CMV-luc (MOI = 3) at E/T ratios of (**F**) 1:2 and (**G**) 1:5. After 3 days, luciferase activity was measured. Results from an experiment representative of 2 independent experiments are shown and statistical analysis was performed using Tukey's multiple comparisons test.

One week after NSG mice were intrasplenically injected with PBMCs from HIV-seronegative donor HGLK055 (20 × 10⁶ cells/mouse) alone or combined with intravenous injection of pp65-αCD28-synTac (4 mg/kg), we intrasplenically injected them with MRC-5 fibroblast cells (5 × 10⁵ cells) 1 day after vitro infection with CMV-luc (MOI of 5). Three days later, the spleens were harvested and divided equivalently for flow cytometric analysis to quantify pp65-specific CD8⁺ T cells and CMV infection (Figure 8A). As described above, in vivo treatment of the mice with pp65-αCD28-synTac (4 mg/kg) markedly expanded the pp65-specific CD8⁺ T cells population by more than 25-fold from an average of less than 1% in the untreated mice to an average of approximately 25% in the αCD28-synTac–treated mice (Figure 8B). This expansion was associated with a significant ($P = 0.009$) approximately 64% reduction in the average CMV infection in the spleens of αCD28-synTac–treated mice as compared with untreated mice (Figure 8C).

We also examined the capacity of SL9-specific CD8⁺ T cells expanded by in vivo treatment with SL9-αCD28-synTac to suppress in vivo emergence of HIV infection following reactivation of latent HIV-infected T cells, mimicking ART interruption in ART-suppressed individuals. We used a humanized mouse model we previously described consisting of NSG mice intrasplenically injected with PBMCs from long-term ART-suppressed HIV-infected donors. We utilized this model to evaluate the capacity of treatments to inhibit the initiation of in vivo plasma viremia associated with the reactivation of latently infected cells in the absence of ART (37). While we observed in vivo expansion of the HIV-SL9–specific CD8⁺ T cell population in the spleens of SL9-αCD28-synTac–treated NSG mice intrasplenically injected with PBMCs from HIV-seropositive donor 619 (Figure 7, F and G), we were unable to evaluate the in vivo capacity of the expanded HIV-SL9–specific CD8⁺ T cells to suppress HIV infection because NSG mice injected with PBMCs from donor 619 did not consistently develop viremia. To circumvent this limitation and our inability to identify another ART-suppressed HIV seropositive donor whose PBMCs both contained HIV-SL9–specific CD8⁺ T cells and produced in vivo viremia after intrasplenic injection in NSG mice, we coinjected PBMCs from donor 619 (32 × 10⁶ cells) with CD8⁺ T cell–depleted PBMCs (14 × 10⁶ cells) from another ART-suppressed HLA-A*0201 donor (donor HGLK67), which lack HIV-SL9–specific CD8⁺ T cells but consistently produce in vivo viremia after intrasplenic injection in NSG mice. After intrasplenic injection of these cells, one group of mice ($n = 7$ mice) was left untreated while another group of mice ($n = 6$ mice) was treated with intravenous injection of SL9-αCD28-synTac (0.4 mg/kg; Figure 8D). We treated the mice with a lower dose of SL9-αCD28-synTac (0.4 mg/kg) because, as shown in Supplemental Figure 3, it expanded SL9-specific CD8⁺ T cells at equivalent to improved levels as compared with treatment with the higher dose (4 mg/kg). After 14 days, the mice were bled to quantify plasma viremia and sacrificed 3 days later to quantify the fraction of SL9-specific CD8⁺ T cells in the mouse spleens. The mean level of plasma viremia in the SL9-αCD28-synTac–treated mice was 73% lower ($P = 0.063$) than the mean level of plasma viremia in the untreated mice (Figure 8E). This was associated with a highly significant ($P = 0.003$) more than 30-fold expansion of the SL9-specific CD8⁺ T cell population in the spleens of SL9-αCD28-synTac–treated mice (mean = 12.1% ± 5.2%) as compared with the SL9-specific CD8⁺ T cell population in

the untreated mouse spleens (mean = 0.36% ± 0.25%; Figure 8F). These data demonstrate the capacity of in vivo synTac treatment to expand pp65- and SL9-specific CD8⁺ T cells capable of suppressing in vivo CMV and HIV infection, respectively.

Discussion

Herein, we describe the activity and function of the highly modular synTac platform consisting of c-pMHC modules covalently linked to costimulatory binding partners, which selectively deliver peptide-specific TCR activation either alone or combined with costimulatory signals to robustly stimulate ex vivo and in vivo activation, expansion, and/or differentiation of primary SL9- and pp65-specific CD8⁺ T cells. SynTacs are engineered as highly stable bivalent Fc fusion proteins to enhance their avidity and to potentially leverage additional Fc-associated effector functions and the antigen-specific delivery of other payloads (e.g., imaging modalities, toxins, affinity reagents) to CD8⁺ T cells. Notably, despite the absence of a linked ligand capable of delivering a costimulatory signal, SL9-FLAG-synTac and pp65-FLAG-synTac treatment markedly expanded primary SL9-specific and pp65-specific CD8⁺ T cells, respectively. It was possible that SL9-FLAG-synTac– and pp65-FLAG-synTac–induced expansion of SL9-specific and pp65-specific CD8⁺ T cells depended on costimulatory signals delivered by adjacent activated APCs and/or by APCs recruited and activated by the binding of the synTac Fc domain to their FcγR. By demonstrating that pp65-FLAG-synTac treatment of highly purified CD8⁺ T cells lacking APCs markedly expanded the pp65-specific CD8⁺ T cell population (Supplemental Figure 3), we established that the delivery of TCR signal alone was sufficient to drive proliferation of pp65-specific CD8⁺ T cells. This behavior may be due to the decreased requirement of memory CD8⁺ T cells for additional costimulatory signals besides the TCR signal to activate and drive proliferation (38–40). A large CMV-specific effector memory CD8⁺ T cell population is maintained after infection (41), as was observed in our donors, and this was the predominant population expanded by synTac stimulation. Similar results were observed in a mouse model where soluble MHC complexes delivering TCR activation signals in the absence of costimulatory stimulation prompted antigen-specific T cell responses (42).

The modular design of synTacs facilitates efficient coupling of diverse costimulatory or coinhibitory ligands with the same c-pMHC to delineate the ex vivo and in vivo effects of different comodulatory signals on antigen-specific T cell function. Additionally, synTacs can be designed to selectively deliver cytokines, such as IL-2, IL-7 and IL-15, which modulate antigen-specific CD8⁺ T cells (43). Because multiple synTacs with identical c-pMHC modules but possessing distinct modulatory or cytokine domains can bind to a single CD8⁺ T cell, they may allow for a reductionist approach to determine how T cell function is differentially modulated by discrete costimulatory and/or cytokine signals. For example, simultaneous CD28 and OX40 costimulation rescues CCR7neg effector T cells from spontaneous and activation-induced cell death, while increasing their antitumor activity (44). GITR costimulation synergizes with B7-CD28 costimulation by lowering the threshold for CD28 costimulation in CD8⁺ T cells (45). CD27 and 4-1BB costimulation synergize to stimulate CD8⁺ effector and memory T cell differentiation (46). Several studies have investigated the differential impact of CD28 versus 4-1BB costimulated signaling on chimeric antigen receptor-T
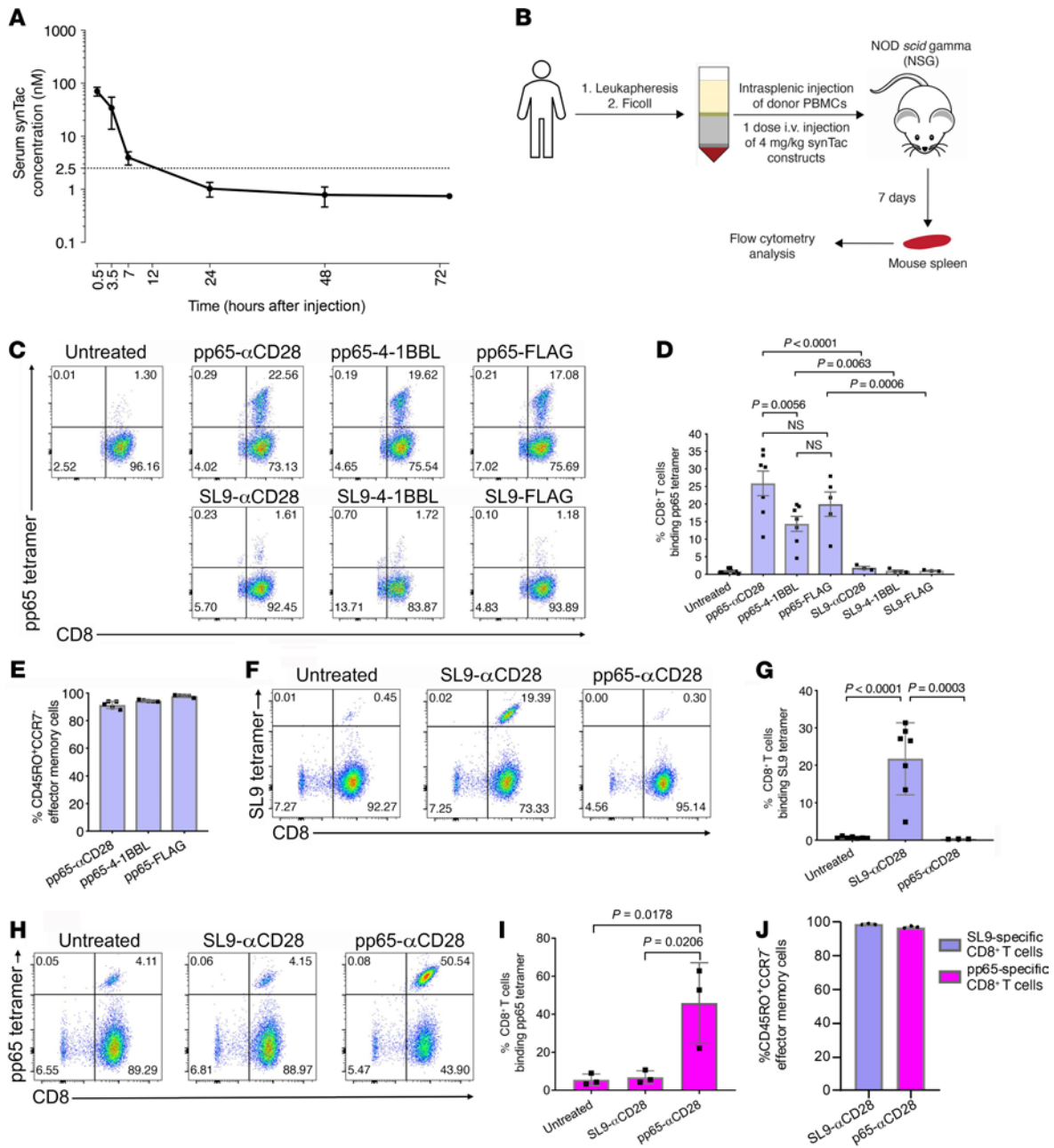
Figure 7. In vivo pp65- or SL9-synTac treatment stimulates expansion of pp65- and SL9-specific CD8+ T cells from HIV-seronegative and -seropositive donors in a humanized mouse model. (**A**) pp65-4-1BBL-synTac serum levels at indicated time points after intravenous injection ($n = 5$ mice) measured by ELISA and presented as mean ± SD. (**B**) Experimental design. (**C**) NSG mice intrasplenically injected with HGLK055 PBMCs were untreated or intravenously injected with the indicated synTacs (4 mg/kg) and after 1 week, the spleens were analyzed by flow cytometry and gated for viability and expression of human CD45 and CD8. (**D**) pp65-specific CD8+ T cells in the spleens of mice that were untreated ($n = 8$) or treated with pp65-αCD28-synTac ($n = 7$), pp65-4-1BBL-synTac ($n = 7$), pp65-FLAG- synTac ($n = 5$), SL9-αCD28 synTac ($n = 3$), SL9-4-1BBL synTac ($n = 3$), or SL9-FLAG synTac ($n = 3$). Shown are pooled data from more than 3 independent experiments statistically analyzed using 1-way ANOVA followed by Tukey's multiple comparisons test. (**E**) Fraction of pp65-specific CD8+ T cells in the spleens of humanized mice treated with the indicated synTac shown in **C**, which were effector memory (CD45RO+CCR7−) cells. (**F**–**J**) NSG mice were intrasplenically injected with PBMCs from HIV-seropositive donor 619 and untreated or intravenously injected with SL9-αCD28-synTac or pp65-αCD28-synTac. One week later, spleens were analyzed by flow cytometry. Dot plots represent SL9 (**F**) or pp65 (**H**) tetramer staining from a representative mouse from each group. (**G**) Summary of the percentage of SL9-specific CD8+ T cells in the spleens of mice that were untreated ($n = 7$) or treated with SL9-αCD28 synTac ($n = 7$) or pp65-αCD28-synTac ($n = 3$). (**I**) Summary of the percentage of pp65-specific CD8+ T cells in the spleens of mice that were untreated or treated with SL9-αCD28-synTac or pp65-αCD28-synTac ($n = 3$/group). Statistical significance was determined by ordinary 1-way ANOVA followed by Tukey's multiple comparisons test. (**J**) Percentage of SL9-specific CD8+ T cells or pp65-specific CD8+ T cells, which were effector memory (CD45RO+CCR7−) cells in the spleens of mice treated with SL9-αCD28-synTac ($n = 3$ mice) or pp65-αCD28-synTac ($n = 3$ mice), respectively shown in **G** and **I**.
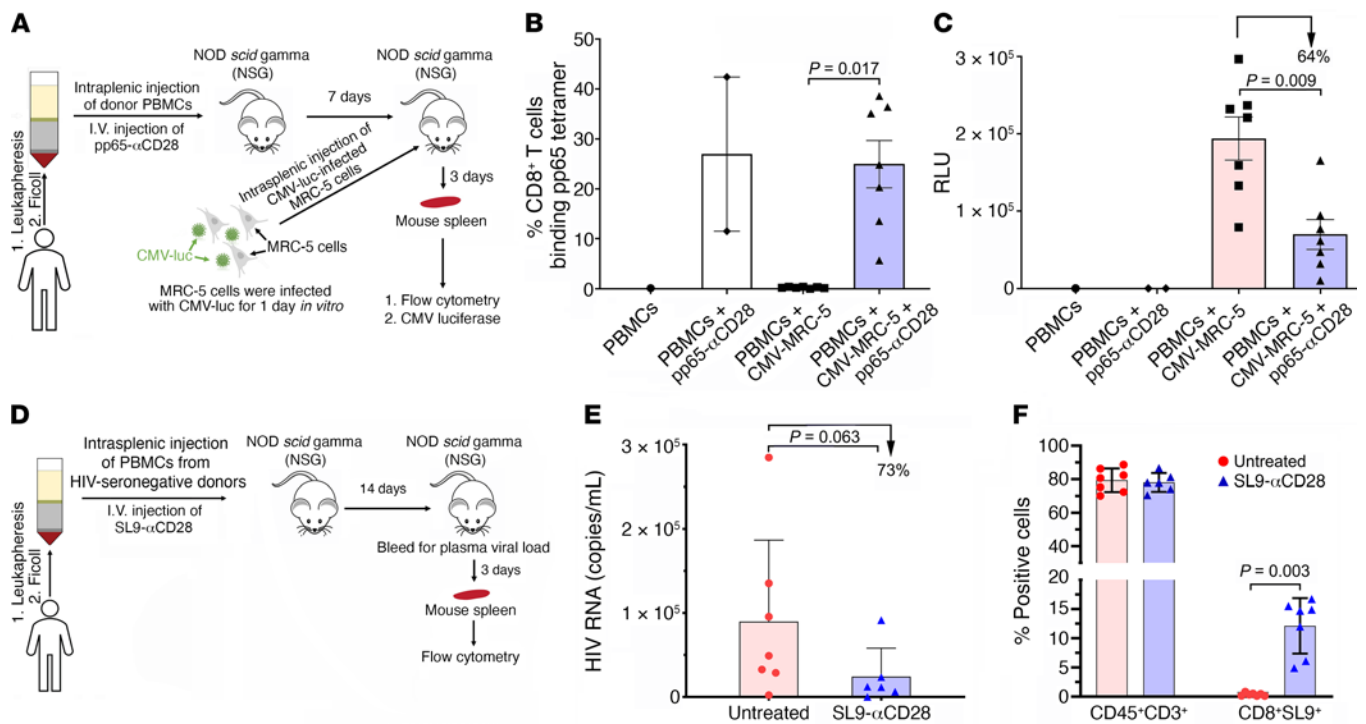
Figure 8. In vivo treatment with synTac expands pp65- and SL9-specific CD8+ T cells and inhibits in vivo CMV and HIV infection. (**A**) NSG mice (*n* = 17 mice) intrasplenically injected with HGLK055 PBMCs were untreated (*n* = 8 mice) or intravenously injected with pp65-αCD28-synTac (4 mg/kg, *n* = 9 mice). One week later, CMV-luc–infected MRC-5 cells were intrasplenically injected into the indicated mice. On day 10, the mouse spleens were harvested to quantify (**B**) pp65-specific CD8+ T cells by flow cytometry and (**C**) CMV infection by luciferase quantification. Dot plots in **B** and **C** show percentage of pp65-specific CD8+ T cells and CMV luciferase levels in the mouse spleens and mean ± SEM, respectively, with percentage of suppression versus untreated mice shown. (**D**) NSG mice (*n* = 13 mice) intrasplenically injected with PBMCs (32 × 10⁶) from HIV-seropositive donor 619 and CD8+ T cell–depleted PBMCs (14 × 10⁶) from donor HGLK67 were untreated (*n* = 7 mice) or intravenously treated with SL9-αCD28-synTac at 0.4 mg/kg (*n* = 6 mice). The mice received no ART. Two weeks later the mice were bled and 3 days later the mouse spleens were harvested. (**E**) HIV viral loads in the plasma were quantified and values for each mouse are shown with mean ± SEM for the untreated and SL9-αCD28-synTac–treated mice and percentage of reduction of the plasma HIV viral loads in the SL9-αCD28-synTac–treated mice as compared with the untreated mice. (**F**) The percentage of human CD45+CD3+ and CD8+ SL9-specific T cells in the spleens of each mouse are shown with mean ± SEM for the untreated and SL9-αCD28-synTac–treated mice. Statistical significance was determined by the Wilcoxon Mann-Whitney *U* test.

(CAR-T) cell function (47). For example, 4-1BB costimulated CAR-T cells display enhanced persistence and frequency of central memory T cells as compared with CD28-costimulated CD19-targeted CAR-T cells (48–50), as well as less cytokine release syndrome and immune effector cell–associated neurotoxicity in treated patients (51, 52).

On potential advantage of synTac-induced immune responses as compared with injection with a mix of peptides and adjuvants which expands antigen-specific T cell populations using multiple costimulatory signals, is that synTacs can induce specific expansion of antigen-specific T cell populations using defined costimulatory signals, which may selectively activate and expand a more long-lived and functional virus-specific T cell population.

Another potential advantage of synTac treatment is that in contrast to broadly antigenic HIV vaccines, which may preferentially expand CD8+ T cells specific for immunodominant but less protective epitopes (53, 54), synTacs may selectively expand CD8+ T cells specific for subdominant but highly conserved HIV epitopes with potent and broad activity that may not be induced by vaccination. While SL9 was selected as the HIV epitope for this proof-of-concept study, the modular design of the synTac construct enables expeditious swapping of peptide and MHC domains to stimulate expansion of CD8+ T cells specific for other more highly conserved epitopes

presented by other MHC class I molecules. The emergence of immune escape mutations over time will require stimulation of a broad CTL response to clear latently infected T cells (55). Treating patients with a combination of synTacs directed at different epitopes, including the highly conserved HIV epitopes identified and validated by other investigators (16, 56, 57), and predicted immune escape mutants, should enable us to generate the broader but focused T cell response needed to overcome the presence or emergence of immune escape variants (58). Alternatively, we could construct synTacs bearing the SL9 variant SLFNTIAVL to stimulate expansion of CD8+ T cells reported to recognize SL9 and other immune escape SL9 variants, which may enable them to eliminate reactivated latent infected cells infected with immune escape variants (59).

The expansion of SL9-specific CD8+ T cells may be hampered by intrinsic limitations in the proliferative capacity of SL9-specific CD8+ T cells (30, 60), which is associated with their increased expression of PD-1 (61). In an HIV-infected donor (donor 619) populated with both SL9- and pp65-specific CD8+ T cells, the SL9-specific CD8+ T cells displayed increased expression of the PD-1 exhaustion marker as compared with pp65-specific CD8+ T cells prior to treatment with synTacs (Figure 4D), perhaps limiting the capacity of SL9-specific CD8+ T cells to be expanded by synTac stimulation.

The expansion of virus-specific CD8+ T cells may also be limited by the reduced CD4+ T cell help provided by the depleted and functionally compromised immune system of HIV infected individuals (62). This factor may account for the markedly lower mean level of expansion of pp65-specific CD8+ T cells induced by pp65-specific synTac treatment of PBMCs from HIV-infected donors (Figure 4B) to less than half the level of expansion induced by pp65-specific synTac treatment of PBMCs from an HIV-uninfected donor (donor HGLK055; Figure 5B).

In contrast to current aAPC approaches for antigen-specific activation of T cells by delivering signal 1 and signal 2, which can only be used for ex vivo T cell expansion and may require aAPC removal prior to in vivo administration of the cells, soluble synTacs could be administered to patients to drive in vivo expansion of endogenous or adoptively transferred antigen-specific CD8+ T cells. SynTacs display potent in vitro activity at concentrations below 1 pM (Figure 5C), enabling synTacs to stimulate in vivo expansion of antigen-specific CD8+ T cells despite their relatively short in vivo half-life of approximately 3 hours in mice (Figure 7A). One week after a single intravenous injection of pp65 synTacs, human pp65-specific CD8+ T cells in the spleens of humanized NSG mice injected intrasplenically with PBMCs from an HIV-seronegative donor expanded to approximately 14% to 25% of the total CD8+ T cell population (Figure 7D). As postulated above for the in vitro studies, the in vivo expansion stimulated by the pp65-FLAG-synTac, which does not deliver a costimulatory signal, may be due to the presence of a large fraction (>60%) of pp65-specific effector memory CD8+T cells in the injected PBMCs, which have a decreased requirement for costimulatory signaling for proliferation in response to antigen-specific TCR stimulation (38–40). Furthermore, in vivo administration of SL9-αCD28-synTac or pp65-αCD28-synTac to humanized mice intrasplenically injected with PBMCs from an HIV-infected donor markedly expanded both the population of SL9-specific CD8+ T cells (Figure 7, F and G) or pp65-specific CD8+ T cells (Figure 7, H and I), respectively, which were predominantly effector memory T cells (Figure 7J). A potential benefit of the relatively short synTac half-life may be a reduction in potential off-target effects in therapeutic applications.

The humanized mouse model employed will support the examination of simultaneous or sequential exposure to various synTacs (e.g., SL9-αCD28-synTac followed by SL9-4-1BBL-synTac and/or SL9-IL-15-synTac) on the stimulation and expansion of naive antigen-specific human CD8+ T cells. A potential limitation of these studies is that the results of synTac treatment in mice intrasplenically injected with human PBMCs may not fully predict the ability of synTacs to stimulate functional CD8+ T cells in patients. However, we demonstrated that primary CD8+ T cells in donor's PBMCs could be selectively expanded by synTacs to yield SL9- and pp65-specific CD8+ T cells capable of potently suppressing in vitro HIV infection (Figure 3E) and CMV infection (Figure 6, F and G), respectively. More notable, we demonstrated that pp65- and SL9-specific CD8+ T cells in donor PBMCs that are selectively expanded in vivo by synTac treatment potently suppressed in vivo CMV infection (Figure 8C) and HIV infection (Figure 8E), respectively. This functional activity supports the potential clinical use of SL9- and pp65-synTacs as a new immunotherapeutic to treat HIV and CMV infection, respectively. The synTac platform combined with the humanized mouse model may also support the development of personalized tumor treatment strategies by evaluating mobilization of immune responses specific for malignancy-associated public (i.e., shared) antigens or distinct neoantigens. Ex vivo immune-phenotyping assays characterizing the responses of a patient's PBMCs to various synTacs could enable the individualized optimization of potential therapeutic strategies with respect to antigenic peptides, modulatory domains, and dosing regimen (e.g., timing, order of addition and synergistic effects), and may provide highly informative biomarkers for stratification and design of tailored therapies for each individual patient.

Methods

Additional details are available in the Supplemental Methods.

Expression and purification of synTac constructs. Expression vectors encoding each component of the SynTac (peptide, β2M, modulatory domain, HLA-A*0201 MHC heavy chain, and Fc domain) flanked by Esp3I Type IIs restriction sites were generated by Golden Gate assembly (63) into the pDaedalus (64) lentiviral vector (FLAG and 4-1BBL synTacs) or a pcDNA 3.1 derivative (αCD28 synTacs) under the human β2M signal peptide. FreeStyle 293-F cells were either transduced with the lentiviral vector or transfected with the pcDNA 3.1 vector and cultured in Freestyle 293 expression media (Gibco). Valproic acid (3 mM) was added to the culture 72 hours before harvest for transduced cells or 24 hours after transfection and synTac protein was purified from clarified culture supernatant by incubation with His60 nickel beads (Takara Bio) and size exclusion chromatography as described (65). Endotoxin levels measured by the Kinetic-QCL LAL assay (Lonza) were typically less than 1 EU/mg purified protein.

Cells. Jurkat/MA cells, a TCR-β chain-deficient Jurkat-derivative engineered to express human CD8α and an NFAT-regulated luciferase reporter gene were obtained from Erik Hooijberg (VU University Medical Center, Amsterdam, The Netherlands) and cultured as described (24). The HIV Gag SL9-specific CD8+ T cell clone obtained from June Kan-Mitchell (University of Texas at El Paso, El Paso, Texas, USA) was generated and cultured as described (26). PBMCs from HIV-uninfected donors were collected from leukopaks (New York Blood Center) by ficoll density gradient centrifugation. For some experiments, CD8+ T cells were isolated from PBMCs by immunomagnetic sorting using human CD8 microbeads or the CD8+ T cell isolation kit using a cocktail of antibodies to deplete non-CD8+ T cells (Miltenyi Biotec). PBMCs were obtained from HIV-infected donors and uninfected donors by bleeding or leukapheresis.

Animals. NSG (NOD-*scid* IL2Rγ^null) mice were purchased from the Jackson Laboratory and maintained as described (37).

Transduction of Jurkat/MA cells by the SL9-TCR–encoding lentiviral vector for evaluation of synTac binding and function. The lentiviral vectors expressing SL9-specific TCR-α and -β chains or 4-1BB were used to transduce Jurkat/MA cells as described (25).

In vitro antigen-specific T cell stimulation by synTac constructs. PBMCs (5×10^5 cells) in complete IMDM (0.5 mL) were plated into individual wells in a 48-well plate and treated with the indicated synTac construct and concentration for 7 to 12 days with added rhIL-2 (100 U/mL) to support sustained antigen-specific CD8+ T cell expansion (66). The fraction of primary CD8+ T cells binding SL9 tetramer or pp65 tetramer (obtained from NIH Tetramer Core Facility) and expressing phenotype markers was determined by flow cytometry as previously described (24).

Tetramer staining to detect the expression of SL9- or pp65-specific T cell receptors. Tetramer staining was performed as described (25).

Propagation of CMV luciferase virus and in vitro CMV inhibition assay.

Towne strain of CMV was engineered to express luciferase (CMV-luc) under the promoter of a CMV late gene pp28 (UL99) and propagated as previously reported (35).

In vitro HIV inhibition by synTac-stimulated HIV-specific CD8+ T cells. The capacity of synTac-stimulated HIV-specific CD8+ T cells to suppress HIV infection was determined using a modification of a method we previously described (24).

Pharmacokinetic measurement of serum synTac concentration in mice. The pharmacokinetics of intravenously injected synTac were determined using a modification of a method we previously described (45).

In vivo stimulation of pp65-specific CD8+ T cells by synTac constructs in a humanized mouse model. PBMCs (12.5 × 10^6) from an HLA-A*0201 HIV-seronegative donor (donor HGLK0055) or HIV-positive donor (donor 619) were injected into the spleens of NSG mice, followed by immediate intravenous injection of the indicated synTac (4 mg/kg). Seven days later, mice were sacrificed, and their spleens were analyzed by flow cytometry.

Evaluation of in vivo inhibition of CMV infection by pp65-specific CD8+ T cells expanded by in vivo treatment of humanized mice with pp65-αCD28 synTac. After NSG mice were intrasplenically injected with PBMCs (20 × 10^6) from an HLA-A*0201 HIV-seronegative donor (donor HGLK055), one group of mice was left untreated and another group was intravenously injected with pp65-αCD28-synTac (4 mg/kg). One week later, the mice were intrasplenically injected with MRC-5 cells (5 × 10^5) 1 day after they were infected in vitro with CMV-luc (MOI of 5). Three days later, mice were sacrificed, their splenocytes were harvested, and one fraction was analyzed by flow cytometry for expansion of the pp65-specific CD8+ T cell population and another fraction was lysed with Luciferase Assay System lysis buffer (Promega) for 30 minutes while shaking. Luciferase units were measured using a Luminat Plus luminometer (Berthold Technologies) to quantify CMV infection.

Evaluation of in vivo inhibition of HIV infection by SL9-specific CD8+ T cells expanded by in vivo treatment of humanized mice with SL9-αCD28 synTac. NSG mice were intrasplenically coinjected with PBMCs containing SL9-specific CD8+ T cells (~32 × 10^6; from an HLA-A*0201 HIV seropositive donor—donor 619) and CD8+ T cell–depleted PBMCs (14 × 10^6; from another HLA-A*0201 HIV-seropositive donor—donor HGLK67) that induce viremia after intrasplenic injection into untreated NSG mice. One group of mice was left untreated and another group was immediately intravenously injected with SL9-αCD28-synTac (0.4 mg/kg). After 14 days, the mice were bled and HIV RNA in the plasma was quantified using a highly sensitive RT-qPCR assay as described (37). Three days later, spleens were harvested and the population of CD8+SL9 tetramer+ cells was quantified as detailed in the Supplemental Methods.

Cytotoxicity assay. Cytotoxic activity of pp65-NLV–specific CD8+ T cells was assessed using DELFIA EuTDA Cytotoxicity Reagents (Perkin-Elmer) and peptide-loaded T2 cells as target cells.

Intracellular cytokine staining. PBMCs or CD8+ T cells were stimulated by peptide-loaded T2 cells in the presence of IL-2 (100 U/mL) and brefeldin A (10 μg/mL, Sigma) and monensin (0.67 μL/mL; BD Biosciences) for 16 hours at 37°C with fluorescently labeled anti-CD107a antibody added at the beginning of the stimulation. The cells were washed with PBS, stained with LIVE/DEAD Blue cell viability dye (ThermoFisher Scientific) and antibodies to phenotypic markers, washed, fixed with 2% paraformaldehyde, and further fixed and permeabilized using the FoxP3/Transcription Factor Staining Buffer Set (eBioscience, ThermoFisher Scientific). The cells were stained with antibodies targeting intracellular cytokines or proteins for 1 hour at room temperature or 4°C overnight. Following staining, cells were washed and analyzed on an LSR II flow cytometer.

Measurement of cytokine production. Secretion of cytokines into cell culture supernatant by synTac-treated CD8+ T cells was quantified with MILLIPLEX MAP Kit (Human CD8+ T-Cell Magnetic Bead Panel, MilliporeSigma) according to the manufacturer's instructions. Cytokine concentrations were measured using Luminex MAGPIX instrument and calculated by the xPONENT software.

Antibodies. To identify lentiviral-encoded gene expression on transduced cells, anti-4-1BB (Biolegend, clone 4B4-1) and anti-hIgG F(ab')2 (Jackson ImmunoResearch, catalog 109-136-098) were used. To identify tetramer-stained CD8+ T cells using flow cytometry, anti-CD3 (Becton Dickinson, catalog 555339), anti-CD4 (Biolegend, catalog 300512), and anti-CD8a (Biolegend, catalog 301032) were used. To determine purity of CD8+ T cells following isolation, anti-CD14 (Biolegend, catalog 325614) and anti-CD56 (Becton Dickinson, catalog 561903) were used. For phenotype marker expression, anti–TNF-α (Biolegend, catalog 502930), anti–IFN-γ (Biolegend, catalog 502512), anti-perforin (Biolegend, catalog 353307), anti-cd107a (Biolegend, catalog 328616), anti-CD28 (Biolegend, catalog 302925), anti–PD-1 (Biolegend, catalog 329905), anti–LAG-3 (Biolegend, catalog 369310), anti–TIM-3 (Biolegend, catalog 369310), anti-CCR7 (BioLegend, catalog 353213), and anti-CD45RO (Biolegend, catalog 304205) were used. To identify human T cells following intrasplenic injection, anti-CD45 (Biolegend, catalog 304014) was used. For the pharmacokinetic ELISA assay, anti–human 4-1BBL antibody (BioLegend, catalog 311502) and anti–human IgG (Sigma-Aldrich, catalog AP113P) were used.

Statistics. Statistical analyses were performed using GraphPad Prism version 8.2. To compare differences in various groups, a 1-way or 2-way ANOVA followed by Tukey's multiple comparisons test, a 2-way ANOVA followed by Sidak's multiple comparisons test, or Wilcoxon Mann-Whitney U test was performed. Differences were considered statistically significant if the P value was less than 0.05.

Study approval. Written consent from PBMC donors was obtained using protocols approved by IRBs from the George Washington University, Rockefeller University, and Albert Einstein College of Medicine. Animal research was approved by the Albert Einstein College of Medicine IACUC in adherence to the NIH Guide for the Care and Use of Laboratory Animals (National Academies Press, 2011).

Author contributions

HG, SCA, and ML conceived and planned experiments. SCA, SJG, RJC, and RDS developed, characterized, and optimized the synTac scaffold. HG, SCA, and ML wrote the manuscript. SJG and RAB critically reviewed the manuscript. ML, SJG, KEO, HS, and DML contributed to performing experimental procedures. SJG and AC contributed to synTac production. RAB provided the CMV luciferase virus. RBJ provided PBMCs from HIV-infected donors.

Acknowledgments

Address correspondence to: Harris Goldstein: Forchheimer 408, Albert Einstein College of Medicine, 1300 Morris Park Avenue, New York, New York 10461, USA. Phone: 718.430.2156; Email: harris.goldstein@einsteinmed.org. Or to: Steven Almo, Forchheimer 408, Albert Einstein College of Medicine, 1300 Morris Park Avenue, New York, New York 10461, USA. Phone: 718.430.2746; Email: steve.almo@einsteinmed.org.

1. Wykes MN, Lewin SR. Immune checkpoint blockade in infectious diseases. *Nat Rev Immunol*. 2018;18(2):91–104.

2. Chen L, Flies DB. Molecular mechanisms of T cell co-stimulation and co-inhibition. *Nat Rev Immunol*. 2013;13(4):227–242.

3. Watts TH. TNF/TNFR family members in costimulation of T cell responses. *Annu Rev Immunol*. 2005;23:23–68.

4. Mescher MF, et al. Signals required for programming effector and memory development by CD8+ T cells. *Immunol Rev*. 2006;211:81–92.

5. Curtsinger JM, Mescher MF. Inflammatory cytokines as a third signal for T cell activation. *Curr Opin Immunol*. 2010;22(3):333–340.

6. Tang Q, et al. CD28/B7 regulation of anti-CD3-mediated immunosuppression in vivo. *J Immunol*. 2003;170(3):1510–1516.

7. Butler MO, Hirano N. Human cell-based artificial antigen-presenting cells for cancer immunotherapy. *Immunol Rev*. 2014;257(1):191–209.

8. Maus MV, et al. Ex vivo expansion of polyclonal and antigen-specific cytotoxic T lymphocytes by artificial APCs expressing ligands for the T-cell receptor, CD28 and 4-1BB. *Nat Biotechnol*. 2002;20(2):143–148.

9. Oelke M, et al. Ex vivo induction and expansion of antigen-specific cytotoxic T cells by HLA-Ig-coated artificial antigen-presenting cells. *Nat Med*. 2003;9(5):619–624.

10. Perica K, et al. Nanoscale artificial antigen presenting cells for T cell immunotherapy. *Nanomedicine*. 2014;10(1):119–129.

11. Schutz C, et al. Antigen-specific T cell redirectors: a nanoparticle based approach for redirecting T cells. *Oncotarget*. 2016;7(42):68503–68512.

12. Tang L, et al. Enhancing T cell therapy through TCR-signaling-responsive nanoparticle drug delivery. *Nat Biotechnol*. 2018;36(8):707–716.

13. Cheung AS, et al. Scaffolds that mimic antigen-presenting cells enable ex vivo expansion of primary T cells. *Nat Biotechnol*. 2018;36(2):160–169.

14. Brockman MA, et al. Challenges and opportunities for T-cell-mediated strategies to eliminate HIV reservoirs. *Front Immunol*. 2015;6:506.

15. Shan L, et al. Stimulation of HIV-1-specific cytolytic T lymphocytes facilitates elimination of latent viral reservoir after virus reactivation. *Immunity*. 2012;36(3):491–501.

16. Sung JA, et al. Expanded cytotoxic T-cell lymphocytes target the latent HIV reservoir. *J Infect Dis*. 2015;212(2):258–263.

17. Patel S, et al. T-cell therapies for HIV: preclinical successes and current clinical strategies. *Cytotherapy*. 2016;18(8):931–942.

18. Mitaksov V, et al. Structural engineering of pMHC reagents for T cell vaccines and diagnostics. *Chem Biol*. 2007;14(8):909–922.

19. Mori M, et al. HLA gene and haplotype frequencies in the North American population: the National Marrow Donor Program Donor Registry. *Transplantation*. 1997;64(7):1017–1027.

20. Ogg GS, et al. Quantitation of HIV-1-specific cytotoxic T lymphocytes and plasma load of viral RNA. *Science*. 1998;279(5359):2103–2106.

21. Diamond DJ, et al. Development of a candidate HLA A*0201 restricted peptide-based vaccine against human cytomegalovirus infection. *Blood*. 1997;90(5):1751–1767.

22. Grosse-Hovest L, et al. A recombinant bispecific single-chain antibody induces targeted, supra-agonistic CD28-stimulation and tumor cell killing. *Eur J Immunol*. 2003;33(5):1334–1340.

23. Bartkowiak T, Curran MA. 4-1BB agonists: multi-potent potentiators of tumor immunity. *Front Oncol*. 2015;5:117.

24. Flerin NC, et al. T-cell receptor (TCR) clonotype-specific differences in inhibitory activity of HIV-1 cytotoxic T-cell clones is not mediated by TCR alone. *J Virol*. 2017;91(6):e02412–16.

25. Joseph A, et al. Lentiviral vectors encoding human immunodeficiency virus type 1 (HIV-1)-specific T-cell receptor genes efficiently convert peripheral blood CD8 T lymphocytes into cytotoxic T lymphocytes with potent in vitro and in vivo HIV-1-specific inhibitory activity. *J Virol*. 2008;82(6):3078–3089.

26. Kan-Mitchell J, et al. The HIV-1 HLA-A2-SLYNT-VATL is a help-independent CTL epitope. *J Immunol*. 2004;172(9):5249–5261.

27. Pollok KE, et al. Inducible T cell antigen 4-1BB. Analysis of expression and function. *J Immunol*. 1993;150(3):771–781.

28. Riou C, et al. Increased memory differentiation is associated with decreased polyfunctionality for HIV but not for cytomegalovirus-specific CD8+ T cells. *J Immunol*. 2012;189(8):3838–3847.

29. Seay K, et al. In vivo activation of human NK cells by treatment with an interleukin-15 superagonist potently inhibits acute in vivo HIV-1 infection in humanized mice. *J Virol*. 2015;89(12):6264–6274.

30. Shankar P, et al. Impaired function of circulating HIV-specific CD8(+) T cells in chronic human immunodeficiency virus infection. *Blood*. 2000;96(9):3094–3101.

31. Adachi K, et al. Cytomegalovirus urinary shedding in HIV-infected pregnant women and congenital cytomegalovirus infection. *Clin Infect Dis*. 2017;65(3):405–413.

32. Lichtner M, et al. Cytomegalovirus coinfection is associated with an increased risk of severe non-AIDS-defining events in a large cohort of HIV-infected patients. *J Infect Dis*. 2015;211(2):178–186.

33. McLane LM, et al. Differential localization of T-bet and Eomes in CD8 T cell memory populations. *J Immunol*. 2013;190(7):3207–3215.

34. Wang Y, et al. Inhibition of cytomegalovirus replication with extended-half-life synthetic ozonides. *Antimicrob Agents Chemother*. 2019;63(1):e01735–18.

35. He R, et al. Recombinant luciferase-expressing human cytomegalovirus (CMV) for evaluation of CMV inhibitors. *Virol J*. 2011;8:40.

36. Bardhi A, et al. Potent in vivo NK cell-mediated elimination of HIV-1-infected cells mobilized by a gp120-bispecific and hexavalent broadly neutralizing fusion protein. *J Virol*. 2017;91(20):e00937–17.

37. Flerin NC, et al. Establishment of a novel humanized mouse model to investigate in vivo activation and depletion of patient-derived HIV latent reservoirs. *J Virol*. 2019;93(6):e02051–18.

38. Kaech SM, et al. Effector and memory T-cell differentiation: implications for vaccine development. *Nat Rev Immunol*. 2002;2(4):251–262.

39. Kersh EN, et al. TCR signal transduction in antigen-specific memory CD8 T cells. *J Immunol*. 2003;170(11):5455–5463.

40. Suresh M, et al. Role of CD28-B7 interactions in generation and maintenance of CD8 T cell memory. *J Immunol*. 2001;167(10):5565–5573.

41. Klenerman P, Oxenius A. T cell responses to cytomegalovirus. *Nat Rev Immunol*. 2016;16(6):367–377.

42. Kosmides AK, et al. Separating T cell targeting components onto magnetically clustered nanoparticles boosts activation. *Nano Lett*. 2018;18(3):1916–1924.

43. Quayle SN, et al. CUE-101, a novel E7-pHLA-IL2-Fc fusion protein, enhances tumor antigen-specific T-cell activation for the treatment of HPV16-driven malignancies. *Clin Cancer Res*. 2020;26(8):1953–1964.

44. Hombach AA, et al. Adoptive immunotherapy

with redirected T cells produces CCR7- cells that are trapped in the periphery and benefit from combined CD28-OX40 costimulation. *Hum Gene Ther*. 2013;24(3):259–269.

45. Ronchetti S, et al. Glucocorticoid-induced TNFR-related protein lowers the threshold of CD28 costimulation in CD8+ T cells. *J Immunol*. 2007;179(9):5916–5926.

46. Willoughby JE, et al. Differential impact of CD27 and 4-1BB costimulation on effector and memory CD8 T cell generation following peptide immunization. *J Immunol*. 2014;193(1):244–251.

47. Cappell KM, Kochenderfer JN. A comparison of chimeric antigen receptors containing CD28 versus 4-1BB costimulatory domains [published online July 6, 2021]. *Nat Rev Clin Oncol*. https://doi.org/10.1038/s41571-021-00530-z.

48. Long AH, et al. 4-1BB costimulation ameliorates T cell exhaustion induced by tonic signaling of chimeric antigen receptors. *Nat Med*. 2015;21(6):581–590.

49. Li G, et al. 4-1BB enhancement of CAR T function requires NF-κB and TRAFs. *JCI Insight*. 2018;3(18):e121322.

50. Kawalekar OU, et al. Distinct signaling of coreceptors regulates specific metabolism pathways and impacts memory development in CAR T cells. *Immunity*. 2016;44(2):380–890.

51. Zhao X, et al. Efficacy and safety of CD28- or 4-1BB-based CD19 CAR-T cells in B cell acute lymphoblastic leukemia. *Mol Ther Oncolytics*. 2020;18:272–281.

52. Ying Z, et al. Parallel comparison of 4-1BB or CD28 co-stimulated CD19-targeted CAR-T cells for B cell non-Hodgkin's lymphoma. *Mol Ther Oncolytics*. 2019;15:60–68.

53. Im EJ, et al. Protective efficacy of serially up-ranked subdominant CD8+ T cell epitopes against virus challenges. *PLoS Pathog*. 2011;7(5):e1002041.

54. Yewdell JW. Confronting complexity: real-world immunodominance in antiviral CD8+ T cell responses. *Immunity*. 2006;25(4):533–543.

55. Deng K, et al. Broad CTL response is required to clear latent HIV-1 due to dominance of escape mutations. *Nature*. 2015;517(7534):381–385.

56. Lam S, et al. Broadly-specific cytotoxic T cells targeting multiple HIV antigens are expanded from HIV+ patients: implications for immunotherapy. *Mol Ther*. 2015;23(2):387–395.

57. Patel S, et al. Functionally active HIV-specific T cells that target Gag and Nef can be expanded from virus-naïve donors and target a range of viral epitopes: implications for a cure strategy after allogeneic hematopoietic stem cell transplantation. *Biol Blood Marrow Transplant*. 2016;22(3):536–541.

58. Douek DC, et al. A novel approach to the analysis of specificity, clonality, and frequency of HIV-specific T cell responses reveals a potential mechanism for control of viral escape. *J Immunol*. 2002;168(6):3099–3104.

59. Iversen AK, et al. Conflicting selective forces affect T cell receptor contacts in an immunodominant human immunodeficiency virus epitope. *Nat Immunol*. 2006;7(2):179–189.

60. Gaiha GD, et al. Dysfunctional HIV-specific CD8+ T cell proliferation is associated with increased caspase-8 activity and mediated by necroptosis. *Immunity*. 2014;41(6):1001–1012.

61. Day CL, et al. PD-1 expression on HIV-specific T cells is associated with T-cell exhaustion and disease progression. *Nature*. 2006;443(7109):350–354.

62. Day CL, Walker BD. Progress in defining CD4 helper cell responses in chronic viral infections. *J Exp Med*. 2003;198(12):1773–1777.

63. Sanjana NE, et al. A transcription activator-like effector toolbox for genome engineering. *Nat Protoc*. 2012;7(1):171–192.

64. Bandaranayake AD, et al. Daedalus: a robust, turnkey platform for rapid production of decigram quantities of active recombinant proteins in human cell lines using novel lentiviral vectors. *Nucleic Acids Res*. 2011;39(21):e143.

65. Ingram JR, et al. PD-L1 is an activation-independent marker of brown adipocytes. *Nat Commun*. 2017;8(1):647.

66. D'Souza WN, Lefrancois L. IL-2 is not required for the initiation of CD8 T cell cycling but sustains expansion. *J Immunol*. 2003;171(11):5727–5735.